



Astrocyte Reaction to Catechol-Induced Cytotoxicity Relies on the Contact with Microglia Before Isolation

Julita Maria Pereira Borges^{1,2} · Lívia Bacelar de Jesus¹ · Cleide dos Santos Souza¹ · Víctor Diogenes Amaral da Silva¹ · Silvia Lima Costa¹ · Maria de Fátima Dias Costa¹ · Ramon Santos El-Bachá¹

Received: 9 January 2022 / Revised: 26 May 2022 / Accepted: 31 May 2022 / Published online: 16 June 2022
© The Author(s), under exclusive licence to Springer Science+Business Media, LLC, part of Springer Nature 2022

Abstract

Astrocytes preserve the brain microenvironment homeostasis in order to protect other brain cells, mainly neurons, against damages. Glial cells have specific functions that are important in the context of neuronal survival in different models of central nervous system (CNS) diseases. Microglia are among these cells, secreting several molecules that can modulate astrocyte functions. Although 1,2-dihydroxybenzene (catechol) is a neurotoxic monoaromatic compound of exogenous origin, several endogenous molecules also present the catechol group. This study compared two methods to obtain astrocyte-enriched cultures from newborn Wistar rats of both sexes. In the first technique (P1), microglial cells began to be removed early 48 h after primary mixed glial cultures were plated. In the second one (P2), microglial cells were late removed 7 to 10 days after plating. Both cultures were exposed to catechol for 72 h. Catechol was more cytotoxic to P1 cultures than to P2, decreasing cellularity and changing the cell morphology. Microglial-conditioned medium (MCM) protected P1 cultures and inhibited the catechol autoxidation. P2 cultures, as well as P1 in the presence of 20% MCM, presented long, dense, and fibrillary processes positive for glial fibrillary acidic protein, which retracted the cytoplasm when exposed to catechol. The *Ngf* and *Il1beta* transcription increased in P1, meanwhile astrocytes expressed more *Il10* in P2. Catechol decreased *Bdnf* and *Il10* in P2 cultures, and it decreased the expression of *Il1beta* in both conditions. A prolonged contact with microglia before isolation of astrocyte-enriched cultures modifies astrocyte functions and morphology, protecting these cells against catechol-induced cytotoxicity.

Keywords Astrocytes · Microglia · Catechol · *Ngf* · *Bdnf* · Neurotoxicity

Statement of Significance Astrocytes play relevant biochemical functions and protection of the nervous system. Astrocyte-enriched primary cultures contribute for understanding physiological and pathological responses, but we must be cautious, since interactions with other cells *in vivo* may modify these responses. Microglial cells may modulate astrocyte functions by secreting several molecules. This work investigated and confirmed the hypothesis that astrocytes early separated from microglia in cultures present different responses to catechol-induced cytotoxicity in comparison to those that stayed with microglia for a longer time. Probably interactions between astrocytes and microglia protect the central nervous system against the toxicity of endogenous and exogenous catechol molecules.

✉ Julita Maria Pereira Borges
jmpborges@uesb.edu.br

✉ Ramon Santos El-Bachá
ramon@ufba.br

Extended author information available on the last page of the article

Introduction

Astrocytes have an important function on the homeostasis of the central nervous system (CNS) (Ballabh et al. 2004). These cells establish a communication bridge between cerebrovascular endothelial cells and neurons. On the other hand, microglia are immunomodulatory cells of the CNS in the presence of pathogens. In fact, astrocyte dysfunction may play a role in the pathophysiology of several disorders (Ricci et al. 2009).

Catechols are molecules that have at least one aromatic ring with two adjacent hydroxyl groups attached to carbons, involved in several pathological conditions in which astrocytes play important roles. Biochemical and structural changes occur in aging subcortical astrocytes, as well as in astroglial cultures subjected to oxidative stress (OS), which may explain many pathological features of Parkinson's

disease (PD) and other neurodegenerative conditions (Schipper et al. 1998). Catechols oxidize at physiological pH, generating reactive toxic species. The catecholamines norepinephrine and epinephrine were toxic to adult rat oligodendrocytes at concentrations of 100 μ M after 5 days of exposure due to hydrogen peroxide production, but these cells were protected when co-cultured with astrocytes (Noble et al. 1994). Catechol estrogens and dopamine oxidize like other catechols. Dopamine undergoes oxidation and cyclization catalyzed by tyrosinase (EC 1.14.18.1), generating aminochrome, which inhibits the proteasome (Zafar et al. 2006), and activates astrocytes and microglia (Santos et al. 2017). Quinones like those derived from estrogen form deoxyribonucleoside adducts (Belous et al. 2007). Glial mitochondrial iron promotes the oxidation of catechol-containing compounds to potentially neurotoxic *ortho*-semiquinone radicals (Schipper 2004). Therefore, these findings motivated us to study the astrocyte reactivity against 1,2-dihydroxybenzene (catechol) oxidation. The toxicodynamic of catechol in glioblastoma cells leads to deoxyribonucleic acid (DNA) fragmentation and apoptosis (de Oliveira et al. 2010). Since catechol is a metabolite of benzene, which is a common pollutant, it is important to understand its toxicity to glial cells. Chemically, catechol differs from catecholamines because it just has the aromatic ring with two adjacent hydroxyl groups, which are also present in all other catechols, but it has not any other chain. These data explain the scientific rationale to use catechol in this work.

Both microglia and astrocytes supposedly play a role in the loss of dopaminergic neurons in PD (Nagatsu and Sawada 2005). Actually, in chronic neurodegenerative diseases, brain tissue is populated with resident inflammatory microglia and astrocytes (Przedborski 2007). Neuroinflammation and OS trigger the release of pro-inflammatory cytokines associated with the activation of microglia and astrocytes (Cai et al. 2011), amplifying the response in a cyclic manner, since both cells mediate more OS (Janda et al. 2012). Indeed, astrocytes may function as a double-edged sword. It seems that the protective role of astrocytes depends on the homeostatic balance between pro-oxidant and protective mechanisms presented by these cells and it may depend on interactions with microglia. Therefore, these data motivated us to study interactions between microglia and astrocytes under stress conditions induced by catechol.

Astrocyte primary cultures have emerged as an important tool for understanding the responses of these cells under both physiological and pathological conditions (Lange et al. 2012). However, astrocytes are not alone in normal as well as in diseased brain, and interactions between astrocytes and microglia in response to catechols are far to be completely understood. Astrocytes in culture can be induced to secrete different cytokines and growth factors, which stimulate the

proliferation of macrophages (Marchetti et al. 1995). BDNF is expressed and secreted by cortical astrocytes in cultures (Seki et al. 2005). Indeed, both astrocytes and microglia respond to neuronal injury and secrete neurotrophic factors (Rajkowska and Miguel-Hidalgo 2007), which can interfere in the function of adjacent cells. Another growth factor that is produced by astrocytes is glial-derived neurotrophic factor (GDNF), which is increased by 1,25-dihydroxy-vitamin D (Cui et al. 2017). Therefore, astrocytes react to changes in their environment by regulating the transcription, translation, and secretion of neurotrophic factors. This is a good reason to investigate the production of neurotrophic factors by astrocyte-enriched cultures when exposed to catechol. This is also important to investigate whether the previous contact with microglia could modulate it.

Currently, the role of microglia on astrocyte injury caused by catechol is unknown. The primary objective of this study intended to challenge astrocyte-enriched cultures with catechol to examine if interactions between astrocytes and microglia before their isolation could protect astrocytes against its toxicity. Therefore, this work investigated the hypothesis that astrocytes, which are early separated from microglia in cultures, present different responses in injury caused by catechol in comparison to those that stayed with microglia for a longer time.

Materials and Methods

Primary Mixed Glial Cultures

Newborn Wistar rats from both sexes were used in the day they were obtained from the animal house of the Laboratory of Neuroscience from the Health Sciences Institute of the Federal University of Bahia. This is emphasized that both sexes were used because most published articles do not specify the sex of animals utilized to prepare primary cultures. Despite the fact that the aim of this work was not to study differences between cultures obtained from male or female newborn rats, it is important to be aware that mixing sex may mask potential differences. The Animal Ethics Committee of the Health Sciences Institute (ICS/CEUA 067/2014) approved the use of 21 newborn rats from both sexes to develop the project. This work is part of this project and used animals based on the assumption that cells obtained from the cerebral cortex of one newborn rat can proliferate to cover 152 cm². Mixed primary glial cell cultures were prepared from cerebral cortices dissected from pups without regard to sex under sterile conditions and freed of their meninges (Cookson and Pentreath 1994). Cells were mechanically dissociated in Dulbecco's modified Eagle's medium (DMEM; Gibco, Grand Island, U.S.A.) with HAM F12 (Gibco, Grand Island, U.S.A.) (1:1, v/v) without serum,

then centrifuged at 2000 g for 10 min. Cells were suspended in DMEM/HAM F12 (1:1, v/v) supplemented with 35 mM sodium bicarbonate (Sigma-Aldrich, St. Louis, USA), 10% (v/v) heat-inactivated fetal calf serum (FCS; Gibco, Grand Island, USA), 100 IU/mL penicillin, and 100 µg/mL streptomycin (Gibco, Grand Island, USA). The cell suspension was plated onto 75 cm² flasks (TPP, Trasadingen, Switzerland). Cells were incubated in a humid atmosphere with 5% CO₂ at 37 °C. Primary astrocyte-enriched cultures can be obtained after mechanically removal of microglia for a review see (Saura 2007). There are two classical procedures to obtain astrocyte-enriched cultures by removing microglia from primary mixed cultures. One of them removes non-adherent cells, including microglia, 48 h after the initial plating of primary mixed cultures (Sidoryk-Wegrzynowicz et al. 2011), and in the other, they are removed after 5–7 days (Kim et al. 2019). Both techniques were used in this work to measure the cytotoxic effects of catechol to astrocytes in order to investigate if the time in which astrocytes and microglia were together in mixed primary cultures could affect it.

Early Microglial Removal

In this procedure (P1), 48 h after the initial plating, flasks were manually and vigorously shaken, in firm horizontal movements, for 2 min to remove microglia and other non-adherent cells from mixed primary cultures. Remained adherent astrocytes were washed 3 times with 0.01 M phosphate-buffered saline, pH 7.4 (PBS), to remove residual culture medium and non-adherent cells, before replacement of the medium. This proceeding was repeated every 48 h until total confluence of astrocytes after 7–10 days. Trypsin (0.25%)

(EC 3.4.21.4; Sigma-Aldrich, St. Louis, USA) and 25% ethylenediaminetetraacetic acid (EDTA, Sigma-Aldrich, St. Louis, USA) in PBS were used to dissociate adherent astrocytes when they attained confluence. Thereafter, astrocytes were seeded at a density of 3×10^4 cells/cm² 24 h prior to experiments. The nuclear chromatin of all cells was stained with 5 µg/mL 2-(4-amidinophenyl)-6-indolecarbamide dihydrochloride (DAPI; Molecular Probes, Eugene, USA) for 10 min at room temperature. Since OX-42 has been applied as a microglial marker (Arai et al. 2003; Jiang et al. 2015; Shin et al. 2012), it was used to investigate their presence.

Late Microglial Removal

In this procedure (P2), mixed primary glial cultures were incubated for 7 days before the first replacement of medium. After primary mixed glial cultures reached confluence (7–10 days), microglial cells were removed by placing flasks in an orbital shaker at 200 rpm during 3 h at 37 °C. Astrocytes that remained attached to flasks after microglial removal were washed with PBS prior to medium replacement. Astrocytes were dissociated from plates with 0.25% trypsin, 25% EDTA in PBS, suspended in DMEM/HAM F12 (1:1, v/v) supplemented with 35 mM sodium bicarbonate, 10% (v/v) FCS, 100 IU/mL penicillin, and 100 µg/mL streptomycin, and seeded at a density of 3×10^4 cells/cm² 24 h prior to experiments. This is important to state that experiments with primary astrocyte-enriched cultures obtained from both described protocols (P1 and P2) were carried out 12 days after initial plating of mixed cultures (Fig. 1).

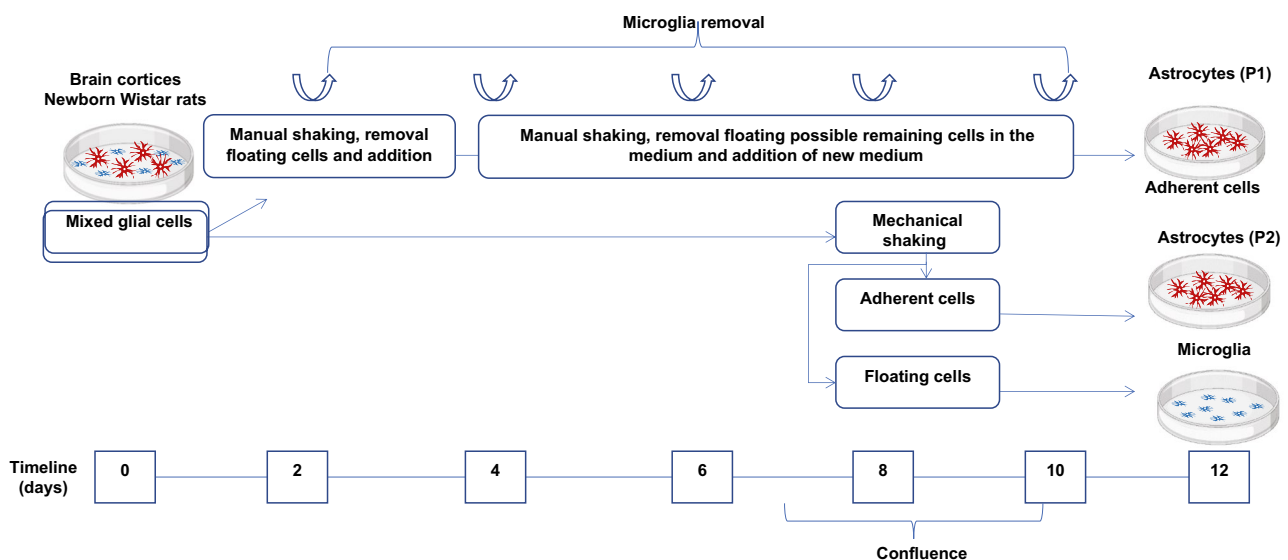


Fig. 1 Timeline of experimental procedures to obtain astrocyte-enriched cultures from primary mixed glial cultures after an early (P1) or late (P2) removal of microglia

Microglial Culture

Microglial isolation was performed according to a technique previously described (Mecha et al. 2011). Floating cells obtained from microglial removal in protocol P2 were centrifuged at 168 g for 10 min. The pellets containing isolated microglia were suspended in DMEM/HAM F12 (1:1, v/v) supplemented with 35 mM sodium bicarbonate, 10% (v/v) FCS, 100 IU/mL penicillin, and 100 µg/mL streptomycin, and incubated in a humid atmosphere with 5% CO₂ at 37 °C. MCM was obtained after 24 h by centrifuging the medium at 532 g for 10 min.

Assessment of Cell Viability

Astrocytes were seeded into 96-well plates (Kasvi, São José dos Pinhais, Brazil) as described in “Early Microglial Removal” and “Late Microglial Removal.” Catechol (Riedel-de Haën, Buchs, Switzerland) was first sublimed at 68 °C in order to be sure of the absence of oxidized molecules, and solutions were prepared in HCl 0.01 M in the day of experiments prior to dilutions, since it oxidizes in neutral aqueous solutions. Experiments were initiated 24 h after plating by adding catechol to the culture medium at 10 different concentrations between 10 and 2000 µM for 72 h ($n=8$ wells for every concentration, including a control group treated only with vehicle). The final HCl concentration was 2×10^{-5} M in all wells containing catechol and the group treated only with the vehicle. Cell viability was measured by the 3-(4,5-dimethylthiazol-2-yl)-2,5-diphenyltetrazolium bromide (MTT; Sigma-Aldrich, St. Louis, USA) test (Mosmann 1983). Data were normalized to the median of absorbances measured at 595 nm for control cells incubated only with medium, without vehicle ($n=7$ wells, since one well was used as a blank without cells). Eight independent experiments were carried out to determine the catechol concentration that killed 50% of cells (EC₅₀) in P1 and P2 cultures. Three independent experiments were carried out for P1 cultures in the presence of MCM. Catechol autoxidation was monitored spectrophotometrically at 405 nm in the medium that was removed prior to the addition of MTT, based on quinone and a melanin-like pigment formation (Lai and Yu 1997). Since quinones, including those formed from catecholamines and their metabolites, absorb light around 400 nm (Ito et al. 2016; Zafar et al. 2006), this enables the observation of the catechol oxidation in cell cultures.

Phenotypic Analysis by Immunocytochemistry

Morphological examination was studied by immunocytochemistry. Astrocytes were evidenced by the presence of GFAP (Hansson 1984; Hughes et al. 2005). Cells were washed three times with PBS and fixed with 4% paraformaldehyde (Sigma-Aldrich, St. Louis, USA) at room

temperature for 20 min. Thereafter, cells were permeabilized with 0.2% (v/v) Triton X-100 (Sigma-Aldrich, St. Louis, USA) in PBS. Bovine serum albumin (Sigma-Aldrich, St. Louis, USA) at 3% (w/v) diluted in PBS served as a blocking reagent. Cells were incubated in a humid chamber at 4 °C overnight with rabbit polyclonal antibody against GFAP (1:300; DAKO, Cat. Number: Z0334, RRID: AB_10013382). Mouse monoclonal antibody against CD11b/c (1:200; Abcam, Cat. Number: ab1211, RRID: AB_442947) was used to investigate the presence of microglia. This antibody recognizes an integrin alpha-M that is the receptor for the iC3b component of complement, also known as OX-42, which is expressed by all dormant and activated rat microglia (Amtul and Hepburn Jeffrey 2014). The next day, cells were rinsed 3 times with PBS, and then incubated with the following secondary antibodies: Goat Alexa Fluor® 488 anti-mouse IgG (1:500; Molecular Probes, Cat. Number: A11001, RRID: AB_2534069) and goat Alexa Fluor® 594 anti-rabbit IgG (1:500; Molecular Probes, Cat. Number: A11012, RRID: AB_141359). Control immunostaining was performed by incubating cells with only secondary antibodies. The nuclear chromatin was stained with 5 µg/mL DAPI for 10 min at room temperature. Coverslips were mounted on slides for observation by confocal microscopy (microscope type TCS SP8, using the Leica Application Suite Advanced Fluorescence software Leica, Wetzlar, Germany) at the Confocal Microscopy Service of the Gonçalo Moniz Research Institute. Excitation was provided by lasers of 405-, 488-, and 559-nm wavelengths.

Control cells were used to assess the morphology of primary astrocytes obtained by both techniques (P1 and P2). Morphological changes were investigated after treatment with 300 µM catechol for 72 h. Thiols like dithiothreitol and L-cysteine completely inhibited the autoxidation of apomorphine (El-Bachá et al. 2001). Furthermore, one detrimental effect of OS is reduced glutathione (GSH) depletion that induces dopaminergic cell death (Kuan and Barker 2005). Therefore, groups of astrocyte-enriched cultures were treated with 300 µM catechol and 3.5 µM GSH (Sigma-Aldrich, St. Louis, USA) in order to investigate the protective effect of this endogenous antioxidant thiol.

Images were acquired from two coverslips per group, and 34–54 cells were examined per experiment. These cells were analyzed by using ImageJ (<https://imagej.nih.gov/ij/download.html>). Cells were morphologically analyzed for the number of processes per astrocyte and measures of their surface area. To mitigate bias in counting, an experimenter blinded to treatment analyzed the pictures. Overlapped cells with not well-defined cytoplasmic delimitation in the plan of the photomicrograph were excluded from counting.

Modulation of Astrocytes Isolated by P1 with Microglial-Conditioned Medium

Astrocyte-enriched cultures obtained after an early removal of microglia were plated in 96-well plates at 3×10^4 cells/cm² in DMEM/HAM F12 (1:1, v/v) supplemented with 35 mM sodium bicarbonate, 10% FCS, 100 IU/mL penicillin, and 100 µg/mL streptomycin, with 20% (v/v) MCM or with 50% (v/v) MCM. These cultures were exposed to catechol at 10 different concentrations between 10 and 2000 µM ($n=8$ wells for every concentration, including incubations only with vehicle, $n=7$ for the control group incubated only with medium because one well was used as a blank without cells) 24 h after plating, and the cell viability was measured by the MTT test after 72 h. Experiments were performed in triplicate.

The cell morphology was studied as described in “Phenotypic Analysis by Immunocytochemistry.” Astrocyte-enriched cultures obtained after an early microglial cell removal were incubated in control conditions, in the presence of 100 µM or 300 µM catechol. Another group was incubated with 20% (v/v) MCM and treated in the same manner. Images were acquired from two coverslips per treatment, and 11–80 cells were examined per experiment. These cells were analyzed by using ImageJ, and they were analyzed as described in “Phenotypic Analysis by Immunocytochemistry.”

RNA Isolation and Quantitation

Total RNA was isolated from cultured astrocytes using TRIzol® (Thermo Fisher Scientific, MA, USA) reagent according to the manufacturer’s instructions. RNA samples were pre-treated with DNase (Ambion DNA-free kit, Life Technologies™, CA, USA) to remove any genomic DNA contamination. A portion of each RNA sample was resuspended in RNA-free ultrapure water and quantified spectrophotometrically at 260 nm. RNA purity was determined using the ratio of absorbance measured at 260 nm and 280 nm (A_{260}/A_{280}).

Quantitative Real-Time Reverse Transcription Polymerase Chain Reaction

cDNA synthesis was performed using the SuperScript® VILO™ Master Mix (Cat. number 11755050, Life Technologies, CA, USA) according to the manufacturer’s protocol. The synthesis was performed in a final volume of 20 µL containing 2.5 µg total RNA. PCR primers for *Bdnf*, *Ngf*, *Gdnf*, *Il10*, *Il1beta*, and the endogenous control, hypoxanthine phosphoribosyl transferase (*Hprt*), were purchased from Thermo Fisher Scientific (MA, USA) (see Table 1 for assay numbers, amplicon lengths, and GenBank accession

Table 1 Target genes in qRT-PCR analysis

Target gene	Amplicon length	ID GenBank	Product code
<i>Ngf</i>	114	FQ232560.1	Rn01533872
<i>Gdnf</i>	122	NC005101.4	Rn01765001
<i>Bdnf</i>	142	AY559248.1	Rn02531967
<i>Hprt</i>	64	NM012583.2	Rn01527840
<i>Il1beta</i>	74	BC091141.1	Rn00580432
<i>Il10</i>	70	L02926.1	Rn00563409

numbers). Quantitative PCR for *Ngf*, *Gdnf*, and *Hprt* were performed using TaqMan® Gene Expression Assays and TaqMan Universal Master Mix II with uracyl-*N*-glycosylase (EC 3.2.2.27) (Applied Biosystems, CA, USA) according to the manufacturer’s protocol. Quantitative PCR was performed using the QuantStudio™ 7 Flex Real-Time PCR System (Applied Biosystems, CA, USA). Amplification conditions were performed according to the manufacturer’s specifications. The analysis of quantitative real-time reverse transcription polymerase chain reaction (qRT-PCR) data was based on the $2^{-\Delta C_t}$ method (Schmittgen and Livak 2008). Tests were performed in triplicate. The expression of *Hprt* was considered as an internal control.

Statistical Analysis

Outlier data points were not excluded prior to analysis. Data were shown as mean with SEM or median with range and 25/75 percentiles according to their distribution, analyzed by the D’Agostino and Pearson normality test, skewness (normal values were considered between -1 and 1), and kurtosis (normal values were considered between -1.5 and 1.5). Also, according to the distribution, parametric or non-parametric statistic tests were chosen. They are indicated in figure legends. Probability values of $p < 0.05$ were accepted as indication of statistically significant difference. Nonlinear regressions were carried out to fit cell viability data in order to determine the catechol concentration that killed 50% of cells (EC_{50}). Analyses were performed by using GraphPad Prism software, version 5.0 for Windows (CA, USA).

Results

Late Removal of Microglia Increased the Resistance of Astrocytes to Catechol-Induced Cytotoxicity

The first experiment shown in this article aimed to observe the catechol cytotoxicity to astrocyte-enriched cultures in which the separation of these cells from microglia occurred early, 48 h after plating of mixed glial primary cultures. The

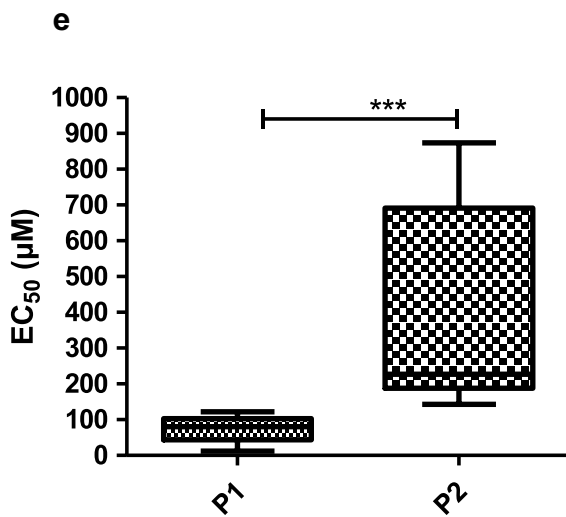
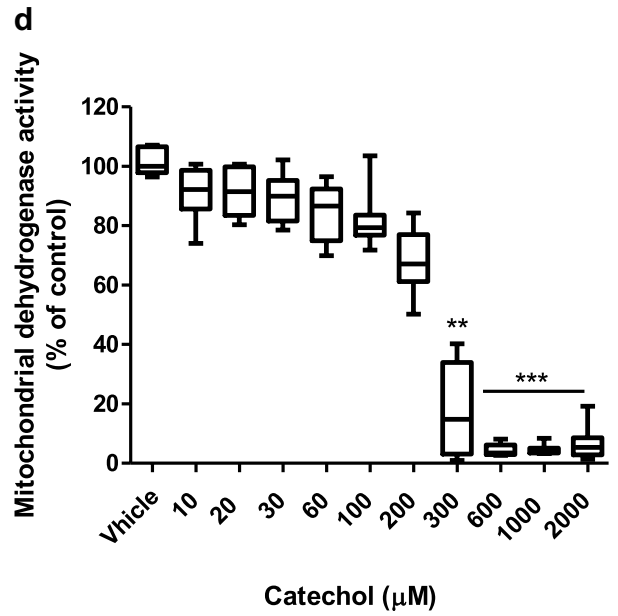
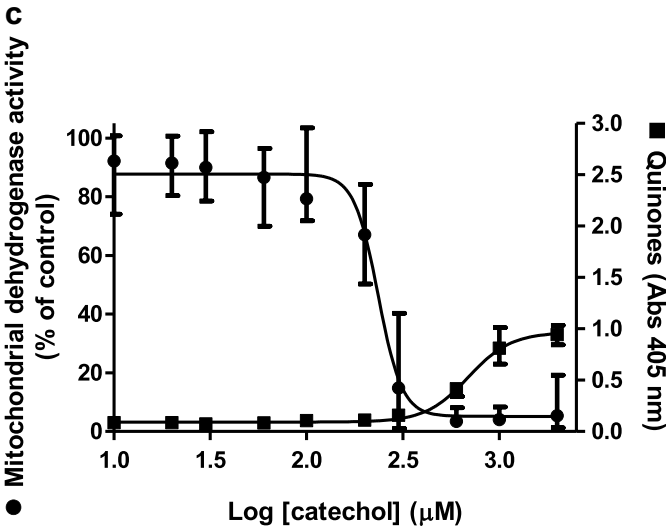
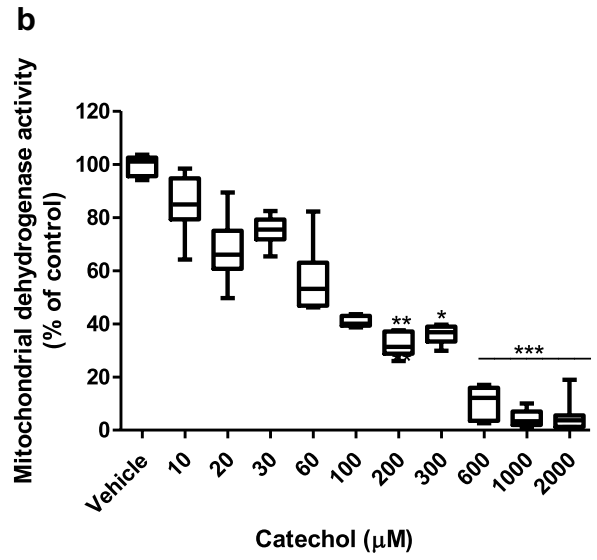
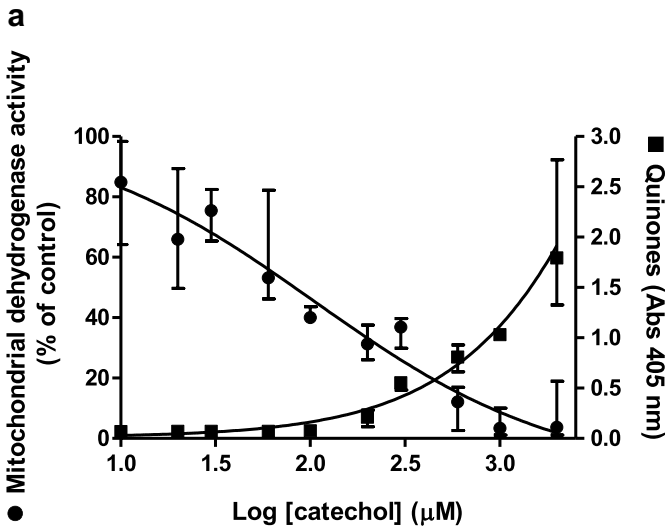


Fig. 2 Cytotoxic effect of catechol to astrocytes and the formation of quinones. **a** Astrocyte-enriched cultures in which microglia were early removed (P1). Data were normalized to the median absorbance measured for control cells incubated only with medium (1.0210, range: 0.9505–1.048, $n=7$ wells), which was considered as 100% viability. Data fitted to a non-linear regression that was used to calculate the EC_{50} . **b** Box plot of cell viability in the same experiment shown in **a**, including the group treated only with the vehicle. **c** Astrocyte-enriched cultures in which microglia were late removed (P2). Data were normalized to the median absorbance measured for control cells incubated only with medium (0.9859, range: 0.9507–1.0560, $n=7$ wells), which was considered as 100% viability. Data fitted to a non-linear regression that was used to calculate the EC_{50} . **d** Box plot of the same data about cell viability shown in **c**, including the control group treated only with vehicle. Cells were incubated with catechol (10–2000 μM) for 72 h in both conditions. Graphs show data from experiments in which EC_{50} corresponded to values nearest to the median of eight independent experiments: 80 μM for P1, and 227 μM for P2. (Filled circle) cell viability; (filled square) quinone formation expressed as absorbances measured at 405 nm. Since data presented non-normal distributions, they were represented by medians and range in **a** and **c** ($n=8$ wells for every concentration, including cells treated only with vehicle), and they were analyzed by Kruskal–Wallis ($p < 0.0001$ for both experiments) followed by Dunn's comparison test. Statistical significance: (*) $p < 0.05$; (**) $p < 0.01$; (***) $p < 0.001$ compared to cells treated only with vehicle (2×10^{-5} M HCl). **e** Comparison between catechol-induced cytotoxicity to astrocyte-enriched cultures obtained after an early removal of microglia (P1) or after a late removal of them (P2). Data represent median EC_{50} values, their ranges, and 25th and 75th percentiles ($n=8$ independent experiments for both groups). Astrocyte-enriched cultures in which microglial cells were late removed were more resistant to catechol than those in which microglial cells were early removed. Groups were compared by the two-tailed Mann–Whitney non-parametric test. Statistical significance: (***) p value: 0.0002. **e** Graphs show data from experiments in which EC_{50} corresponded to values nearest to the median of eight independent experiments: 80 μM for P1, and 227 μM for P2

median EC_{50} value for catechol-induced cytotoxicity to these astrocytes was 80 μM (range: 12–122 μM ; 25/75 percentiles: 44–103; $n=8$ independent experiments). Catechol-induced cytotoxicity to these astrocytes in the experiment in which EC_{50} corresponded to a value nearest to the median (Fig. 2a) fitted to Eq. (1):

$$V = \left\{ 114.30 / \left[1 + 10^{(0.66 \text{Log} C - 1.35)} \right] \right\} - 12.33 \quad R^2 = 0.906 \quad (1)$$

in which V corresponds to cell viability normalized to data measured under control conditions, and C is the catechol concentration. Exposure to catechol for 72 h promoted a significant concentration-dependent cell death in these cultures (Kruskal–Wallis test, $p < 0.0001$; 11 groups; Kruskal–Wallis statistic H 82.54; Fig. 2b). The cytotoxic effect was associated with quinone formation, which resulted from the autoxidation of catechol (Fig. 2a).

Thereafter, another experiment investigated if a prolonged contact between astrocytes and microglia prior to their separation could interfere in catechol-induced cytotoxicity to astrocytes. In these astrocyte-enriched cultures, the separation of these cells from microglia occurred 7 days after plating of glial mixed primary cultures. Catechol treatment

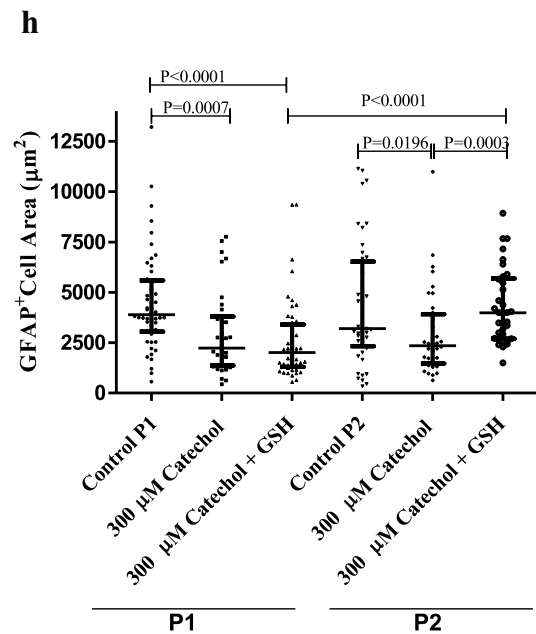
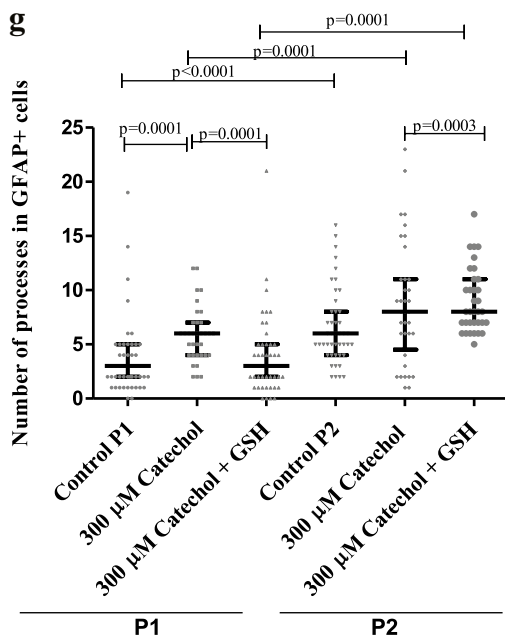
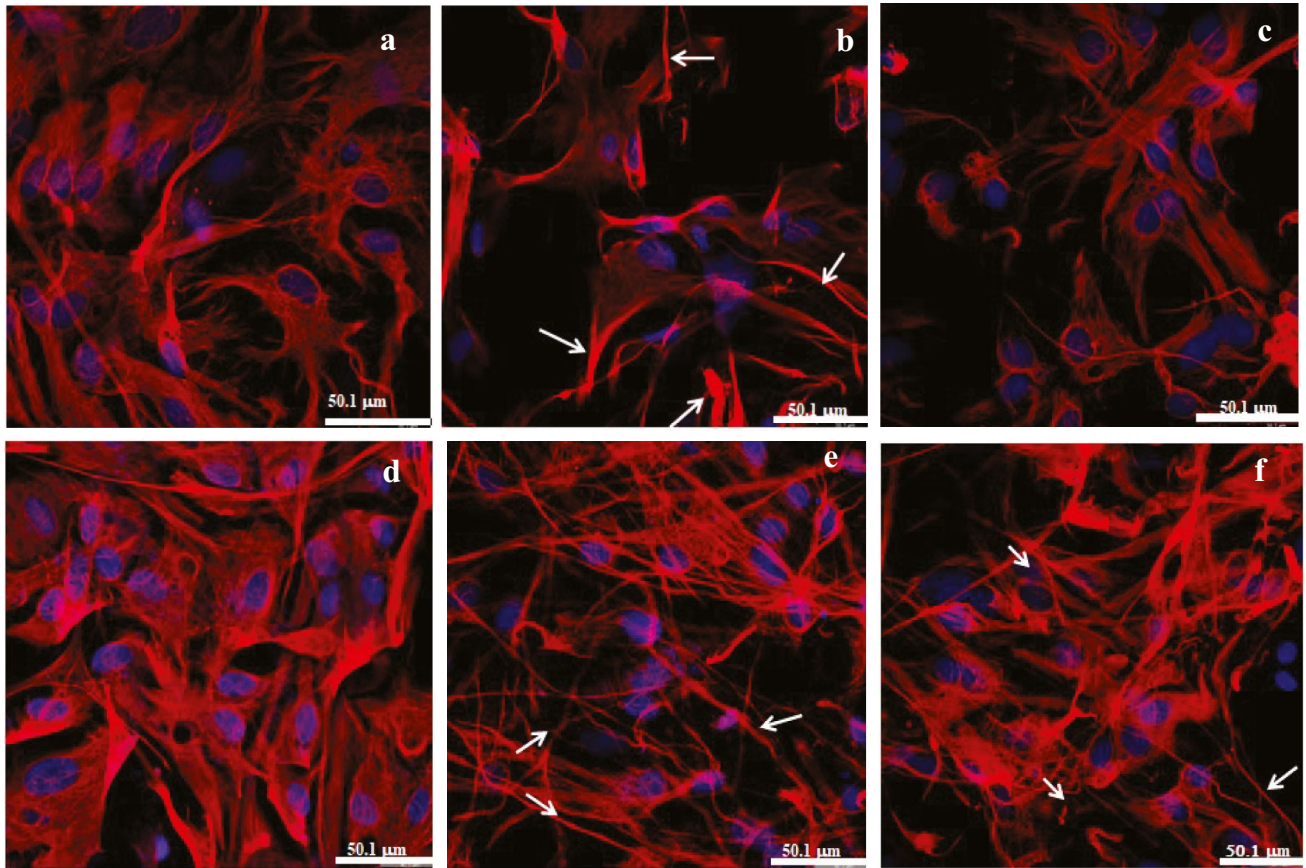
also resulted in cytotoxicity to astrocyte-enriched cultures in which microglia were late removed (P2). However, the median EC_{50} value for catechol-induced cytotoxicity to these astrocytes after 72 h was 227 μM (range: 143–874 μM ; 25/75 percentiles: 188–692; $n=8$ independent experiments). Catechol-induced cytotoxicity to these astrocytes in the experiment in which EC_{50} corresponded to a value nearest to the median (Fig. 2c) fitted to Eq. (2):

$$V = 5.16 + \left\{ 82.58 / \left[1 + 10^{(7.01 \text{Log} C - 16.63)} \right] \right\} \quad R^2 = 0.948 \quad (2)$$

Exposure to catechol for 72 h promoted a significant concentration-dependent cell death in these cultures (Kruskal–Wallis test, $p < 0.0001$; 11 groups; Kruskal–Wallis statistic H 71.05; Fig. 2d). Once more, the cytotoxic effect was associated with quinone formation. There is a significant difference between EC_{50} values. Astrocyte-enriched cultures obtained after a late removal of microglia were more resistant to catechol-induced cytotoxicity when compared to those obtained after an early removal (Fig. 2e).

The Late Removal of Microglial Changes the Astrocyte Morphology Induced by Catechol

Most cells were stained with GFAP, demonstrating the presence of astrocytes in cultures obtained after an early or late removal of microglia (Fig. 3). The red fluorescence was localized in the cytoplasm. Nuclei were stained with DAPI. No microglia were detected in both techniques. This does not mean that these techniques lead to pure astrocyte cultures. Indeed, the aim of this work was not to produce pure cultures, rather it was intended to enrich them with astrocytes, beginning the separation of these cells from microglia early, 48 h after mixed cultures were launched, or late, after 7 days. In control conditions, astrocyte-enriched cultures, in which the removal of microglia began early (P1), presented a polygonal or a spindle-shaped morphology with radiating filamentary processes organized in bundles around a central nucleus (Fig. 3a). Most astrocytes obtained after a late removal of microglia presented a flat and polygonal morphology in control conditions (Fig. 3d). To determine the physiological impact of interactions with microglia prior to isolate astrocytes, morphological changes were quantified by analyzing the number of total astrocyte processes per GFAP⁺ cell. Astrocytes that were late separated from microglia presented significantly ($p < 0.0001$, two-tailed Mann–Whitney test) more processes (median: 6; range: 2–16; 25/75 percentiles: 4–8; $n=45$) than those that were early separated (median: 3; range: 0–19; 25/75 percentiles: 2–5; $n=50$) (Fig. 3g). However, no significant difference on cytoplasmic areas was observed in both conditions (Fig. 3h). The median area of astrocytes that were early separated from microglia was 3891 μm^2 (range: 568–13,218; 25/75 percentiles:



3056–5597; $n = 50$), and in those that were late separated, the median area was $3200 \mu\text{m}^2$ (range: 342–11,145; 25/75 percentiles: 2332–6527; $n = 45$) ($p = 0.4583$, two-tailed Mann–Whitney test).

A decrease in cellularity was observed in astrocyte-enriched cultures obtained after an early removal of microglia when exposed to $300 \mu\text{M}$ catechol for 72 h (Fig. 3b). Moreover, astrocytes presented an apparent increase in long,

Fig. 3 Representative images of the immunocytochemistry of primary astrocyte-enriched cultures obtained after an early (P1) or late (P2) removal of microglia. Astrocytes were labeled by goat Alexa Fluor® 594 (red) anti-rabbit IgG bound to rabbit monoclonal antibody against GFAP. The presence of microglia was investigated by immunolabeling for OX-42 (green). Nuclei were stained by DAPI (blue). **a** Control P1 condition. **b** Astrocytes of P1 cultures treated with 300 μM catechol for 72 h. **c** Astrocytes of P1 cultures treated with 300 μM catechol and 3.5 μM GSH for 72 h. **d** Control P2 condition. **e** Astrocytes of P2 cultures treated with 300 μM catechol for 72 h. **f** Astrocytes of P2 cultures treated with 300 μM catechol and 3.5 μM GSH for 72 h. Cells were analyzed by confocal microscopy. Most cells are positive for GFAP. Microglia were not seen. Arrows indicate fibrillary processes formed by GFAP. Bars are equivalent to 50.1 μm . **g** Analysis of the number of astrocyte processes. **h** Analysis of cell area. Control cells were treated only with vehicle (2×10^{-5} M HCl). Treated cells were exposed to 300 μM catechol alone or in the presence of 3.5 μM GSH for 72 h. Data are shown as scatter plots with medians and interquartile ranges. Control P1 ($n=50$ in **g** and 50 in **h**); control P2 ($n=45$ in **g** and 45 in **h**); Catechol 300 μM P1 ($n=34$); catechol 300 μM P2 ($n=36$); catechol 300 μM +GSH P1 ($n=48$); catechol 300 μM +GSH P2 ($n=34$). Two-tailed Mann–Whitney non-parametric test was used to compare one group with another. Comparisons of the number of astrocyte processes between P1 and P2 cells treated only with catechol, and between P2 treated with catechol alone and P2 treated with catechol+GSH were carried out by using the two-tailed unpaired t test because these groups presented normal distributions

dense, and fibrillary processes positive for GFAP, which retracted their cytoplasm. This was confirmed by analyzing the number of processes per GFAP⁺ cells (median: 6; range: 2–12; 25/75 percentiles: 4–7; $n=34$). There was a significant increase compared to control cells ($p=0.0001$; two-tailed Mann–Whitney test; Fig. 3g). Furthermore, the median area of cells was 2238 μm^2 (range: 437–7760; 25/75 percentiles: 1366–3799; $n=34$). There was a significant retraction of the cytoplasm when compared to correspondent control cells ($p=0.0007$, two-tailed Mann–Whitney test; Fig. 3h). An apparent decrease in cellularity was also observed in astrocyte-enriched cultures obtained after a late removal of microglia when they were treated with 300 μM catechol for 72 h (Fig. 3e). Furthermore, most astrocytes presented GFAP organized in fibrillary processes, which presented significantly more processes (median: 8; range: 1–23; 25/75 percentiles: 4–11; $n=36$) than their correspondent control cells ($p<0.06$; two-tailed Mann–Whitney test; Fig. 3g). Catechol also induced a significant retraction of the cytoplasm, which presented a median area of 2353 μm^2 (range: 640–10,994; 25/75 percentiles: 1468–3919, $n=36$), when compared to respective control cells ($p=0.038$, two-tailed Mann–Whitney test; Fig. 3h). The number of processes per astrocytes treated with 300 μM catechol that were late separated from microglia was also significantly greater than in those also treated, but that were early isolated. Since both treated groups presented normal distributions, they were compared by using the two-tailed unpaired t test (P1 treated with catechol, mean \pm SD: 5.9 ± 2.8 ; P2 treated with

catechol, mean \pm SD: 8.8 ± 1.0 ; $p<0.008$). However, no difference was observed for their cellular areas ($p=0.9766$, two-tailed Mann–Whitney test).

Since catechol cytotoxicity was associated with its oxidation, the effect of the endogenous antioxidant GSH was investigated. GSH at 3.5 μM apparently increased the cellularity and prevented catechol-induced morphological changes in astrocyte-enriched cultures obtained after an early removal of microglia (Fig. 3c). The number of processes per cells (median: 3; range: 0–21; 25/75 percentiles: 2–5; $n=48$) was the same as that observed for control cells ($p=0.6768$; two-tailed Mann–Whitney test; Fig. 3g). However, 3.5 μM GSH significantly decreased the number of processes per GFAP⁺ cells when compared to cells treated only with 300 μM catechol ($p<0.0001$, two-tailed Mann–Whitney test; Fig. 3g). Although cells seemed to be more polygonal than fibrillary, they remained significantly retracted when compared to respective control cells (median area: 2012 μm^2 ; range: 559–9367; 25/75 percentiles: 1305–3401, $n=48$; $p<0.0001$; two-tailed Mann–Whitney test; Fig. 3h). Furthermore, no difference was observed when compared to cells treated only with catechol ($p=0.9766$; two-tailed Mann–Whitney test). In astrocyte-enriched cultures obtained after a late removal of microglia, GSH also increased the presence of astrocytes with a polygonal morphology, but many fibrillary processes were still present (Fig. 3f). Furthermore, GSH did not decrease the number of processes per astrocytic cells when compared with the group treated only with 300 μM catechol. Since these two groups presented normal distributions, they were analyzed by using the two-tailed unpaired t test (P2 treated only with catechol, mean \pm SD: 8.7 ± 0.93 ; P2 treated with catechol+GSH, mean \pm SD: 9.0 ± 0.5 ; $p=0.8184$). However, GSH protected cells against catechol-induced cell retraction ($p=0.0003$, two-tailed Mann–Whitney test; Fig. 3h). Moreover, the number of processes per GFAP⁺ cells in astrocyte-enriched cultures obtained after a late removal of microglia and treated with catechol and GSH was greater than in those obtained after an early removal of microglia and treated in the same manner ($p<0.0001$; two-tailed Mann–Whitney test; Fig. 3g). The cell area in astrocyte-enriched cultures obtained after a late removal of microglia and treated with catechol and GSH was also greater than in those obtained after an early removal of microglia and treated in the same manner ($p<0.0001$; two-tailed Mann–Whitney test; Fig. 3h).

The Microglial-Conditioned Medium Protected Astrocytes Against Catechol-Induced Cytotoxicity

Since astrocyte-enriched cultures obtained after a late removal of microglia presented an increased resistance to catechol, the longer time that these cells remained in contact with microglia before their separation could explain this result. Therefore, cultures obtained after an early removal

of microglia were incubated with MCM and exposed to this compound in order to discover if microglia-secreted factors could interfere on the resistance of astrocytes to catechol. The MCM at 20% significantly increased the median EC_{50} value to 656 μM (range 574–675 μM ; $n=3$ independent experiments; two-tailed Mann–Whitney test, $p<0.05$ compared to P1 described in “Late Removal of Microglia Increased the Resistance of Astrocytes to Catechol-Induced Cytotoxicity,” $n=8$ independent experiments). The experiment in which EC_{50} corresponded to the median (Fig. 6) fitted to Eq. (3):

$$V = 9.44 + \left\{ 56.40 / \left[1 + 10^{(14.52 \text{Log } C - 41.31)} \right] \right\} R^2 = 0.874 \quad (3)$$

This means that the resistance of astrocytes to catechol significantly increased eightfold when compared to astrocyte-enriched cultures obtained after an early removal of microglia in the absence of MCM. A reduction in the absorbance at 405 nm due to quinones formed during catechol autoxidation was also observed (Fig. 4). These data revealed that factors secreted by microglia in the medium play a role in protecting astrocytes against catechol-induced cytotoxicity. Therefore, astrocyte-enriched cultures obtained after an early removal of microglia were incubated in medium with 50% (v/v) MCM

($n=3$ independent experiments), and under this condition, the cytotoxic effect of catechol as well as its autoxidation were completely abolished (Fig. 5).

Morphological Response of Astrocytes to Catechol in the Presence of Microglial-Conditioned Medium

In this experiment, astrocyte-enriched cultures obtained after an early removal of microglia presented an almost confluent monolayer of large and flat polygonal GFAP⁺ cells in control conditions, in the absence of MCM (Fig. 6a). Astrocytes that were early separated from microglia presented a median of 3 processes per GFAP⁺ cells (range: 0–10; 25/75 percentiles: 2–4; $n=62$) (Fig. 6g). The median area was 2554 μm^2 (range: 5086–33,688; 25/75 percentiles: 1311–4601; $n=62$) (Fig. 6h). However, MCM at 20% (v/v) modulated a retraction of the cytoplasm, a loss of the confluence, and some astrocytes began to emit thin fibrillary processes, suggesting that they became reactive (Fig. 6d). Indeed, the number of processes per GFAP⁺ cells (median: 5; range: 1–11; 25/75 percentiles: 3–7; $n=62$) significantly increased when compared to control cells ($p=0.0001$; two-tailed Mann–Whitney test, Fig. 6g). However, the cell area (median: 2813 μm^2 ; range: 784–21,225; 25/75 percentiles: 1896–3733; $n=62$;

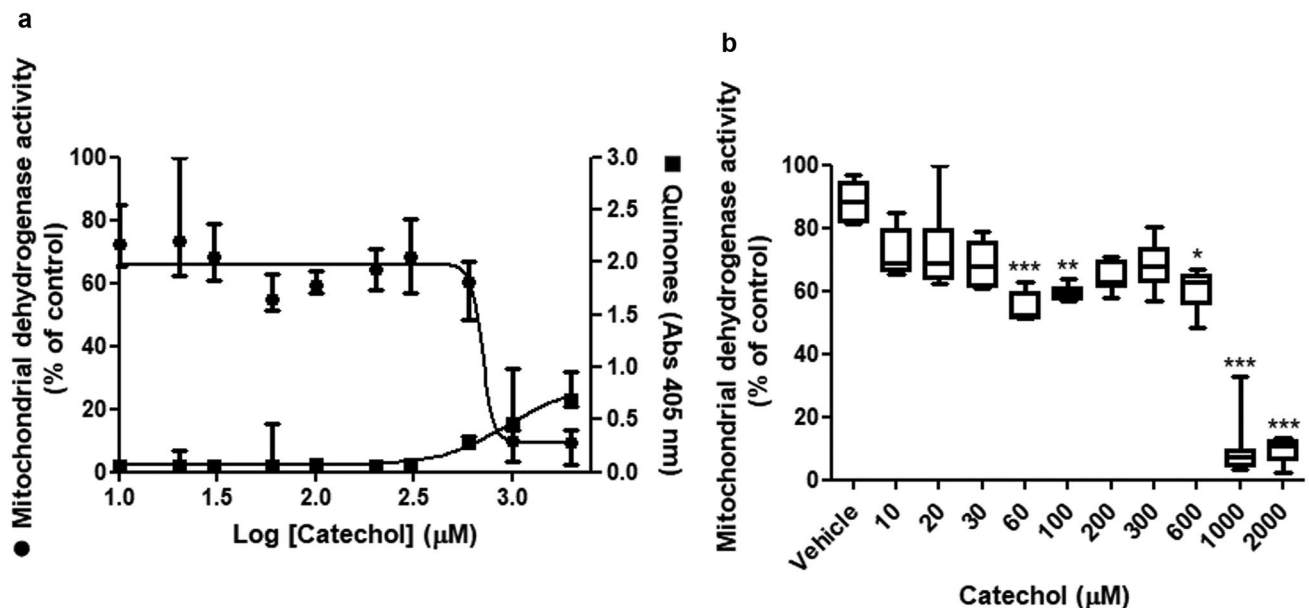


Fig. 4 Cytotoxic effect of catechol to astrocyte-enriched cultures obtained after an early removal of microglia modulated with 20% (v/v) MCM. **a** Data were normalized to the median absorbance measured for control cells incubated only with medium (0.9200, range: 0.8314–0.9872, $n=7$ wells), which was considered as 100% viability. Cells were incubated with catechol (10–2000 μM) or only with vehicle (2×10^{-5} M HCl) for 72 h. The graph shows data from the experiment in which EC_{50} corresponded to the median value: 656 μM . Data fitted to a non-linear regression that was used to calculate the

EC_{50} . (Filled circle) cell viability; (filled square) quinone formation. Since data presented non-normal distribution, they were represented by medians and range ($n=8$ wells for every concentration). **b** Box plot of data about cell viability in the same experiment shown in **a**, including the group treated only with the vehicle. Data were analyzed by Kruskal–Wallis ($p<0.0001$) followed by Dunn’s multiple-comparison test. Statistical significance: (*) $p<0.05$; (**) $p<0.01$; (***) $p<0.001$ compared to cells treated only with vehicle

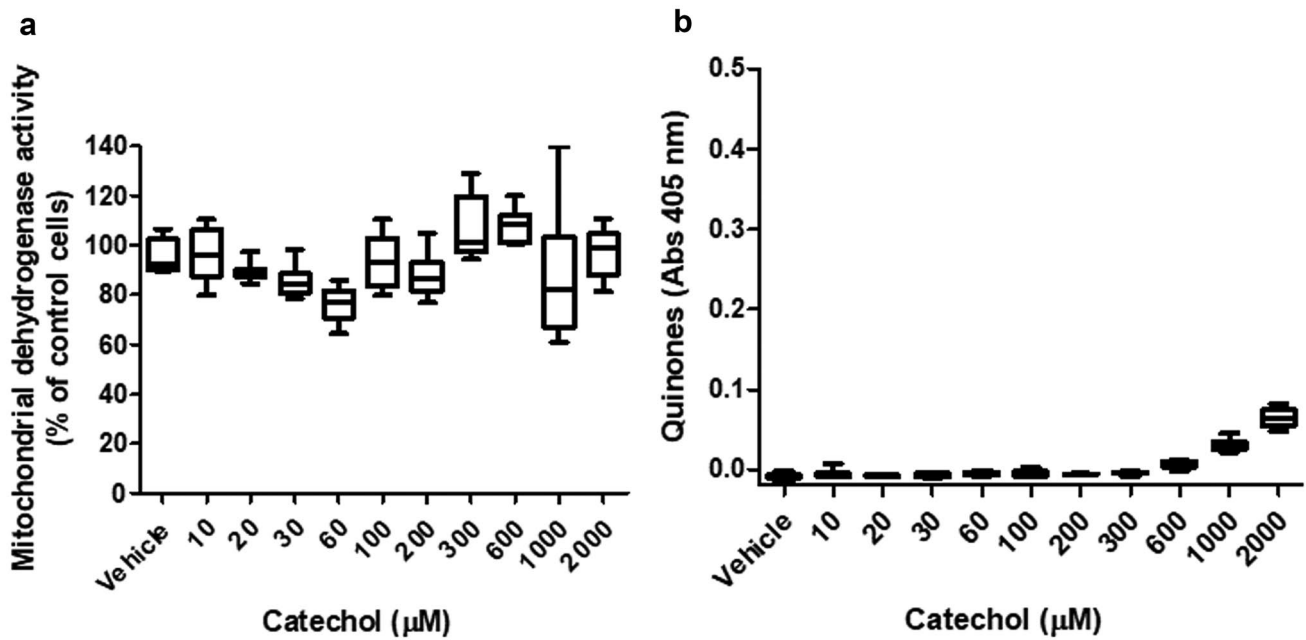


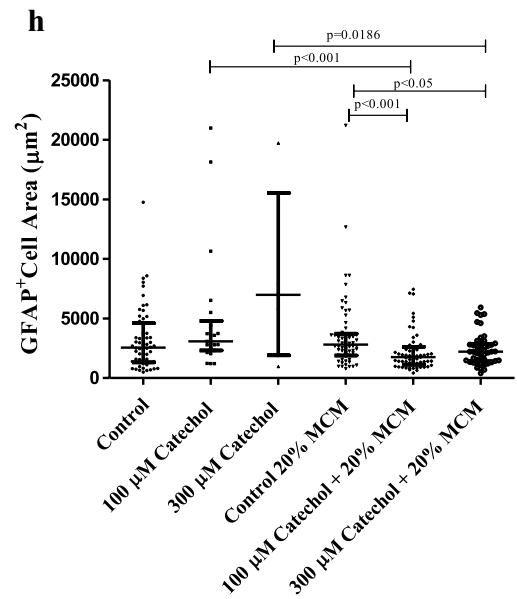
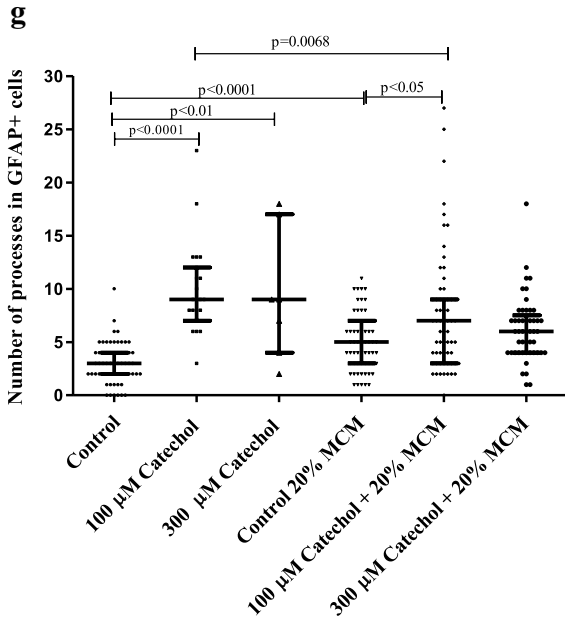
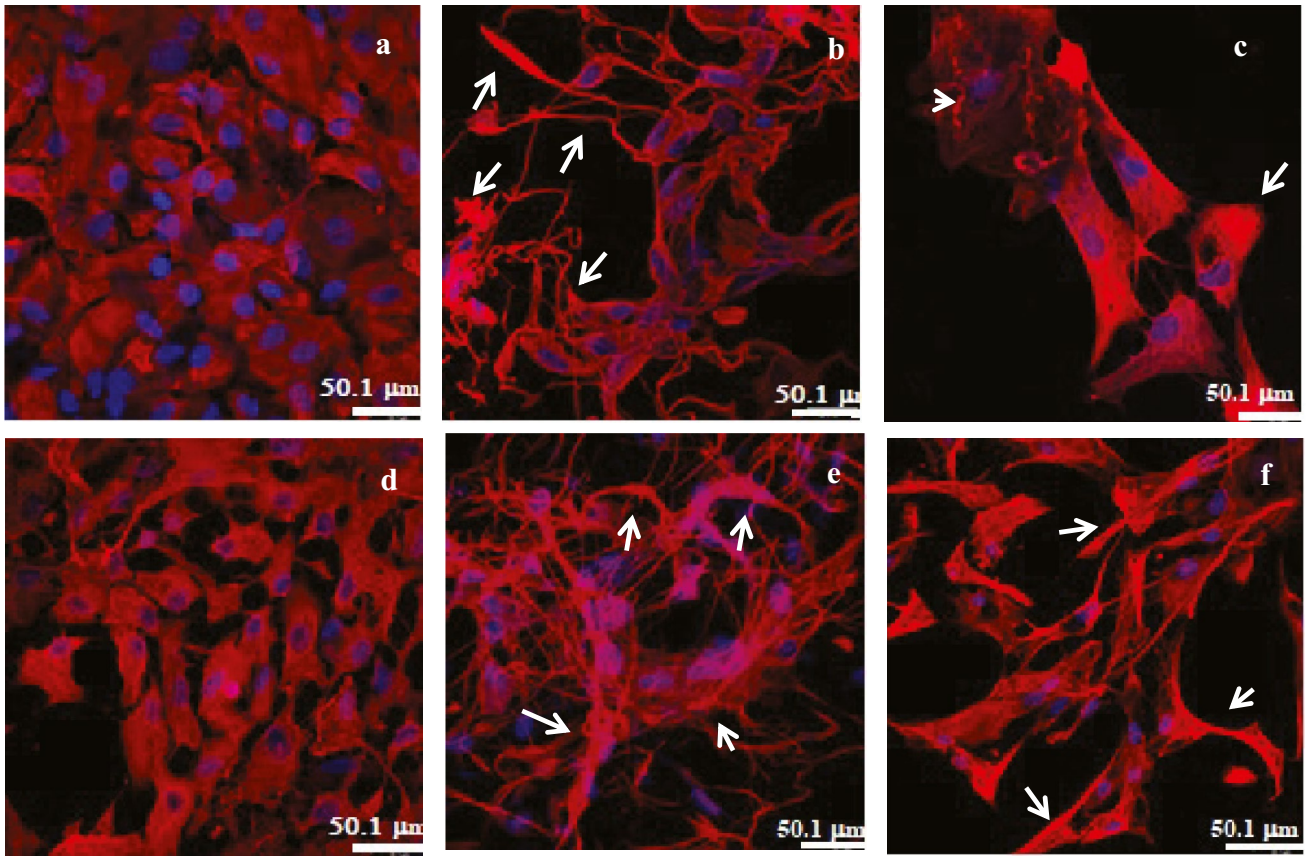
Fig. 5 Evaluation of catechol-induced cytotoxicity to astrocyte-enriched cultures obtained after an early removal of microglia modulated with 50% (v/v) MCM. **a** Cell viability measured by the MTT test. Data were normalized to the median absorbance measured for control cells incubated only with medium (0.5569, range: 0.4846–0.5978, $n=7$ wells), which was considered as 100% viability. Cells were incubated with catechol (10–2000 μM) or only with vehicle

(2×10^{-5} M HCl) for 72 h ($n=8$ wells for every concentration). The graph shows data from one of three independent experiments. **b** Quinone formation. Since data presented non-normal distribution, they were represented by medians and range ($n=8$ wells for every concentration). Data were analyzed by Kruskal–Wallis followed by Dunn’s multiple-comparison test

Fig. 6h) did not differ from control cells ($p=0.2917$; two-tailed Mann–Whitney test). Probably these morphological differences modulated by MCM are related to the increased resistance to catechol.

Catechol at 100 μM decreased the cellularity, and induced morphological changes after 72 h in the absence of MCM (Fig. 6b). Reactive astrocytes retracted their cytoplasm and emitted long, thin, and fibrillary processes, which were strongly immunolabeled for GFAP. Actually, the catechol concentration significantly altered the number of processes per astrocytes in these cultures ($p<0.0001$; Kruskal–Wallis test, Kruskal–Wallis statistics: 47.23). The number of processes per GFAP⁺ cells significantly increased ($p<0.001$; Dunn’s multiple-comparison test; difference in rank sum: –23,12) in astrocytes treated with 100 μM catechol after 72 h (median: 9; range: 3–23; 25/75 percentiles: 7–12; $n=23$; Fig. 6g). The catechol concentration also significantly altered cell areas ($p=0.0443$; Kruskal–Wallis test, Kruskal–Wallis statistics: 6.234), although no difference ($p>0.05$; Dunn’s multiple-comparison test; difference in rank sum: –10.73) was observed in cells treated with 100 μM catechol (median: 3081 μm^2 ; range: 1219–20,978; 25/75 percentiles: 2316–4796; $n=23$; Fig. 6h). The reactivity strongly increased when astrocytes were exposed to 100 μM catechol in the presence of 20% MCM (Fig. 6e). The catechol concentration

significantly altered the number of processes per GFAP⁺ cells ($p=0.026$; Kruskal–Wallis test, Kruskal–Wallis statistics: 7.30). Astrocyte-enriched cultures obtained after an early removal of microglia incubated with 20% MCM and treated with 100 μM catechol presented a median of 7 processes per astrocytes (range: 0–27; 25/75 percentiles: 3–9; $n=63$; Fig. 6g). This was significantly greater than the respective control ($p<0.05$; Dunn’s multiple-comparison test; difference in rank sum: –23.12; Fig. 6g), but this was significantly lesser than the cells incubated with 100 μM catechol in the absence of MCM ($p=0.0068$; two-tailed Mann–Whitney test; Fig. 6g). The catechol concentration also induced a significant alteration in cell areas in the presence of MCM ($p<0.0001$; Kruskal–Wallis test, Kruskal–Wallis statistics: 36.56) (Fig. 6h) cytoplasmic retraction (median area: 1760 μm^2 ; range: 425–35,175; 25/75 percentiles: 1129–2614; $n=63$; Fig. 6h). The exposure to 300 μM catechol induced a great decrease in cellularity in the absence of MCM (Fig. 6c); some cells presented a disorganization of intermediate filaments forming the cytoskeleton. However, the few cells that preserved their structures presented significantly more processes (median: 9; range: 2–18; 25/75 percentiles: 4–17; $n=7$) than their respective control ($p<0.01$; Dunn’s multiple-comparison test; difference in rank sum: –33.72; Fig. 6g). These apparently preserved cells were also significantly



enlarged (median area: 6982 μm^2 ; range: 974–19,726; 25/75 percentiles: 5905–15,532; $n=7$; $p < 0.05$; Dunn’s multiple-comparison test; difference in rank sum: -27.34 ; Fig. 6h). The cellularity was apparently greater in astrocyte cultures

treated with 300 μM catechol in the presence of 20% MCM than in its absence (Fig. 6f). Despite the decrease in cellularity of astrocytes treated with catechol in the presence of MCM when compared to their respective control cells, some

Fig. 6 Representative images of the immunocytochemistry showing the influence of MCM on primary astrocyte-enriched cultures obtained after an early removal of microglia (P1). Astrocytes were labeled by goat Alexa Fluor® 594 (red) anti-rabbit IgG bound to rabbit monoclonal antibody against GFAP. Microglia were immunolabeled for OX-42 (green). Nuclei were stained by DAPI. **a** Control condition in the absence of MCM. **b** Astrocytes treated with 100 μM catechol for 72 h in the absence of MCM. **c** Astrocytes treated with 300 μM catechol for 72 h in the absence of MCM. **d** Astrocytes in the presence of 20% (v/v) MCM. **e** Astrocytes treated with 100 μM catechol for 72 h in the presence of 20% MCM. **f** Astrocytes treated with 300 μM catechol for 72 h in the presence of 20% MCM. Cells were observed by confocal microscopy. Microglia were not seen. Arrows indicate fibrillary processes formed by GFAP. Arrowhead shows disorganization of intermediate filaments forming the cytoskeleton. Bars are equivalent to 50.1 μm . **g** Analysis of the number of astrocyte processes. **h** Analysis of cell area. Control cells were treated only with vehicle (2×10^{-5} M HCl). Treated cells were exposed to 100 μM or 300 μM catechol for 72 h. Data are shown as scatter plots with medians and interquartile ranges. Control cells in the absence of MCM ($n=62$); cells treated with 100 μM catechol in the absence of MCM ($n=23$); cells treated with 300 μM catechol in the absence of MCM ($n=7$); control cells incubated with 20% MCM ($n=62$); cells treated with 100 μM catechol in the presence of MCM ($n=63$); cells treated with 300 μM catechol in the presence of MCM ($n=49$). The Kruskal–Wallis test was used to analyze the effect of catechol concentration in the three groups incubated in the absence, or in the presence of MCM, followed by the Dunn’s multiple-comparison test. Two correspondent groups incubated in the presence or in the absence of MCM were compared by the two-tailed Mann–Whitney test. Values of $p < 0.05$ were considered as significant

of them showed a star-like shape typically presented by reactive astrocytes. However, the median number of processes per astrocytes (median: 6; range: 1–18; 25/75 percentiles: 4–7.5; $n=49$; Fig. 6g) did not differ from the respective control. They were significantly more retracted (median area: 2210 μm^2 ; range: 394–5926; 25/75 percentiles: 1395–2862; $n=49$)

than cells treated with 300 μM catechol in the absence of MCM ($p=0.0187$; two-tailed Mann–Whitney test; Fig. 6h).

The Early Removal of Microglia Increased by Almost Five-Fold the *Ngf* Transcription

In order to verify the transcription of *Gdnf*, *Ngf*, and *Bdnf* in astrocyte-enriched cultures isolated by P1 and P2 protocols, as well as the effect of catechol on these expressions, we performed a qRT-PCR analysis. There was no difference in the transcription of *Gdnf* between both methods that were used to obtain astrocyte-enriched cultures (Fig. 7a). Furthermore, catechol did not interfere in the expression of this gene in both cultures. On the other hand, the transcription of *Ngf* was 4.9 times greater in astrocyte-enriched cultures obtained after an early removal of microglia than in those obtained after a late removal (Fig. 7b). The absence of statistical significance must be considered cautiously. The probability of normal distributions should not be tested for small samples ($n < 8$). Therefore, a nonparametric analysis was carried out ($n=3$ for every group). Catechol did not modify the expression in both conditions. The transcription of *Bdnf* was similar in both culture protocols, but catechol significantly decreased the gene expression of this neurotrophic factor in astrocyte-enriched cultures obtained after a late removal of microglia ($p=0.04$; Kruskal–Wallis test, Kruskal–Wallis statistic: 6.489) (Fig. 7c).

Catechol Decreased *Il10* Transcription After a Late Removal of Microglia

The transcription of *Il1beta* was 1.4-fold greater in astrocyte-enriched cultures obtained after an early removal of

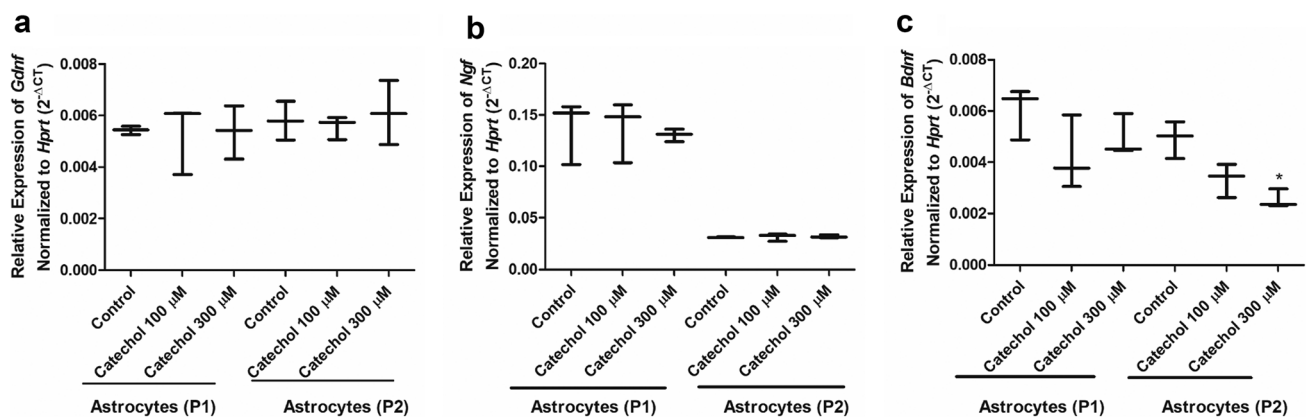


Fig. 7 qRT-PCR for *Gdnf* (a), *Ngf* (b), and *Bdnf* (c) in astrocyte-enriched cultures isolated after early (P1) or late (P2) microglial removal. The effect of treatments with 100 μM or 300 μM for 72 h was also observed. Expression levels were normalized to *Hprt*. Data are shown as medians and ranges of $2^{-\Delta\text{CT}}$ ($n=3$ for every group).

Two sets of measurements were compared by the two-tailed Mann–Whitney test. The effect of catechol concentration was analyzed by the Kruskal–Wallis test followed by Dunn’s multiple-comparison test. (*) $p < 0.05$ compared to the control P2

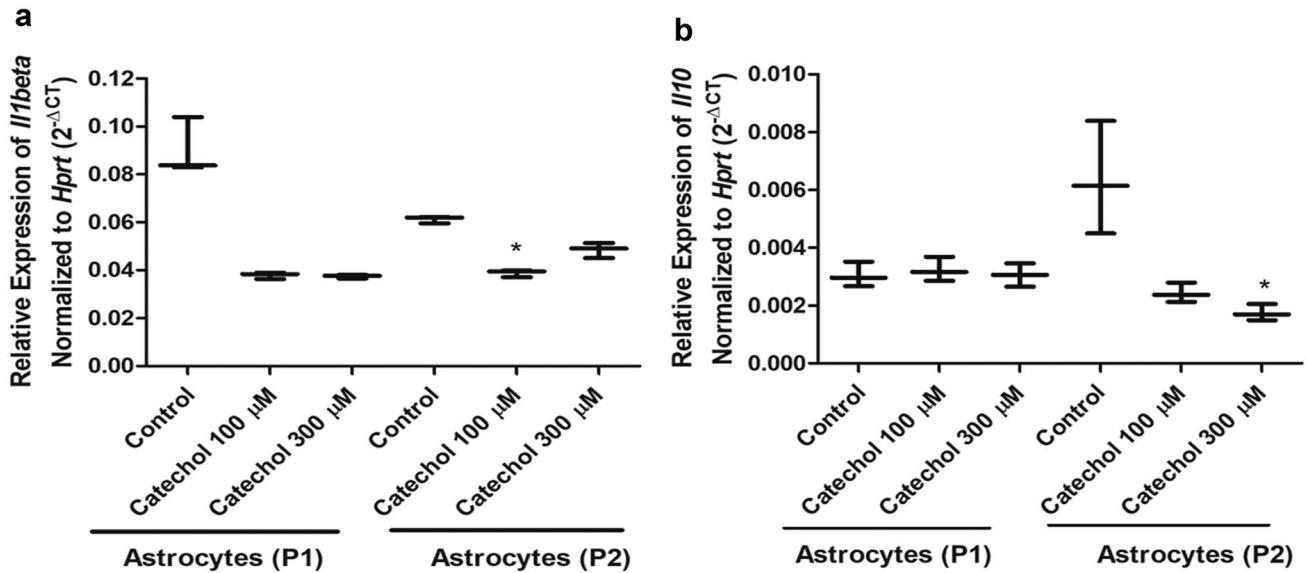


Fig. 8 qRT-PCR for *Illbeta* (a) and *Il10* (b) in astrocyte-enriched cultures isolated after an early (P1) or late (P2) microglial removal. The effect of treatments with 100 μ M or 300 μ M catechol for 72 h was also observed. Expression levels were normalized to *Hprt*. Data are shown as medians and ranges of $2^{-\Delta CT}$ ($n=3$). Two sets of meas-

urements were compared by the two-tailed Mann–Whitney test. The effect of catechol concentration was analyzed by the Kruskal–Wallis test followed by Dunn’s multiple-comparison test. (*) $p < 0.05$ compared to the control P2

microglia compared to those obtained after a late removal (Fig. 8a), but it was not significant by using the nonparametric test. Despite the fact that catechol decreased the transcription of *Illbeta* by 2.2-fold in astrocyte-enriched cultures obtained after an early removal of microglia, the nonparametric Kruskal–Wallis test showed no significant effect. However, a significant effect was found for the catechol treatment in astrocyte-enriched cultures obtained after a late removal of microglia, in which it decreased the transcription by 1.6-fold.

The transcription of *Il10* is twofold greater in astrocyte-enriched cultures obtained after a late removal of microglia compared to those obtained after an early removal (Fig. 8b). However, the absence of statistical significance of the nonparametric test must be considered cautiously. Catechol did not modulate the *Il10* expression in astrocyte-enriched cultures obtained after an early removal of microglia (P1). However, catechol significantly decreased the *Il10* expression in astrocyte-enriched cultures obtained after a late removal of microglia (P2).

Discussion

The data presented in this paper show that the time in which astrocytes remained together with microglia in primary mixed glial cultures prior to their isolation to obtain astrocyte-enriched cultures influenced their resistance to catechol-induced cytotoxicity. Data

evidenced that astrocyte-enriched cultures obtained after a late removal of microglia were more resistant to catechol than astrocyte-enriched cultures obtained after an early removal of these cells. Moreover, the data indicated that the time in which astrocytes remained together with microglia also influenced alterations in their morphology when challenged by catechol. The results presented here highlight these effects, since MCM protected astrocyte-enriched medium obtained after an early removal of microglia. The time of contact with microglia prior to the isolation of astrocyte-enriched cultures also modulated the transcription of *Ngf*, which increased almost fivefold in astrocyte-enriched medium obtained after an early removal of microglia compared to cultures obtained after a late removal of microglia. However, the transcription of *Il10* increased twofold in astrocyte-enriched cultures obtained after a late removal of microglia compared to those obtained after an early removal.

Curiously, when primary astrocyte-enriched cultures were obtained by magnetic cell sorting, which uses microbeads conjugated to an antibody against OX-42 to eliminate microglia, there was a decrease in the GFAP expression (Losciuto et al. 2012). The functional neurovascular unit of the CNS is formed by endothelial cells, pericytes, the basement membrane, astrocytes, neurons, microglia, and oligodendrocytes (Sá-Pereira et al. 2012). Astrocytes separated late from microglia by the second method uptake more acrylonitrile than these latter cells (Caito et al. 2013). Could

the astrocyte-conditioned medium modify the microglial uptake, and vice versa? Astrocyte-enriched cultures obtained after a late removal of microglia produce galectin-9 when stimulated with IL-1 β , TNF, and interferon (IFN)- γ (Steelman et al. 2013). Two different astrocyte fractions can be separated by sedimentation field flow fractionation, in which the purest one presented smaller cells with a tendency to aggregate (Sarrazay et al. 2013). Could MCM modify this morphology? The extracellular matrix is another factor that can influence cellular behaviors (Chen et al. 2015), which limits in vitro observations. In addition, astrocytes of aged BALB/c mice express more *Gfap* mRNA in the hippocampus and cerebellum than adult animals (Norden et al. 2016). Therefore, age is another important factor that is associated with changes in astrocyte morphology and function. However, the majority of studies carried out in vitro use astrocyte-enriched cultures from newborn animals, which limits our understanding. Primary cells also may lose their phenotype in culture (Potjewyd et al. 2018). Astrocytes histologically observed in biological tissues are morphologically different from those observed in cultures. Therefore, despite the importance of in vitro and in vivo studies, extrapolations of their findings to the human disease should be done cautiously (Hornedo-Ortega et al. 2018). Microglia keep a watch on the brain at the forefront of the neuroinflammatory response in different insults (Eldahshan et al. 2019). However, in the injured or diseased brain, neuro-inflammation is also orchestrated through the activation of astrocytes, neurons, endothelial cells, and pericytes triggered by exogenous and endogenous factors released by challenged cells (Thurgur and Pinteaux 2019).

In this study, astrocyte cultures in which microglia were early removed were more sensitive to catechol-induced cytotoxicity than cultures in which these cells were late removed. The median EC₅₀ in early removal (82 μ M) was lesser than that obtained for a primary mixed glial culture (342 μ M) (Almeida et al. 2007). On the other hand, the median EC₅₀ in late removal (229 μ M) is comparable to that found in a primary mixed glial culture. It seems that the contact between microglia and astrocytes in mixed primary cultures during cell expansion prior to their separation influences the resistance to catechol. However, since the resistance continued even after the late removal of microglia, this suggests that changes occurred in astrocytes lasted after their separation. Toxicity in glial cells disturbs a normal response to challenges, which amplifies damages to neurons (Ghatak et al. 2018), and might have major impacts on the function of neuronal circuits (Juricek and Coumoul 2018).

Other catechols are also toxic to glial cells. Apomorphine killed almost 50% of rat glioma C6 cells at 400 μ M after 6 h (El-Bachá et al. 1999). This compound oxidizes like other catechols generating reactive quinones and oxygen species (El-Bachá et al. 2001). In the present work, the catechol

oxidation was greater in the medium when microglia were early removed in comparison to the late removal, and it seems to be associated with its cytotoxicity. Catechol inhibited liver mitochondrial state 2 FADH₂-linked respiration (Barreto et al. 2005). Since the MTT assay measures mitochondrial dehydrogenase activities of alive cells, probably the death of astrocytes may be at least partially due to the inhibition of mitochondrial respiration. 3-Methylcatechol is a toluene metabolite that also oxidizes and inhibited state 2 FADH₂-linked respiration of nonsynaptic mitochondria (Barreto et al. 2007).

The EC₅₀ of catechol-induced cytotoxicity to human glioblastoma GL-15 cells after 72 h varied between 230 and 252 μ M (de Oliveira et al. 2010; Pereira et al. 2004). Therefore, the resistance of astrocytes to catechol-induced cytotoxicity after a late removal of microglia is similar to that found for human glioblastoma cells. However, it seems that astrocytes are more resistant to catechol than cells of a neuronal origin, since the EC₅₀ to neuroblastoma N2a cells was 38 μ M (Lima et al. 2008). Mixed glial cell cultures were also more resistant than neurons to the toxicity induced by alkaloids (Silva et al. 2013). Since astrocytes generally have higher GSH concentrations than neurons (Rae 2014), this could explain their greater resistance to catechol.

Cells in astrocyte-enriched cultures obtained by both methods presented a polygonal or a spindle-shaped morphology, with the prevalence of the former. The same was observed in primary mixed glial cultures, but with the prevalence of the latter morphology (Hansson 1984). The majority of cells presented filaments formed by GFAP as previously described (Schildge et al. 2013). Microglia stain positively for the specific marker OX-42 (Floden and Combs 2007; Mesquita et al. 2014), but their presence was not observed in both methods used to obtain astrocyte-enriched cultures in this work. Antibodies against OX-42 are used efficiently to select and isolate microglial cells for cultures (Bohlen et al. 2017).

Catechol decreased cellularity more in astrocyte-enriched cultures obtained after an early removal of microglia, than in those in which microglia were late removed. Catechol induced a different reorganization of intermediate filaments in astrocyte-enriched cultures obtained after a late removal of microglia compared to the P1 method, suggesting that the contact with microglia prior to separation modulated it. In positive GFAP cells exposed to catechol, this protein formed long and thin fibrillary processes, more evidenced when microglia were late removed. Although no more microglia were present, it seems that they influenced the endurance of astrocytes. Since microglia secrete several growth factors and cytokines that regulate cell maintenance and plasticity (Unsicker et al. 1992), these proteins may have influenced astrocytes which remained in contact with these cells for a longer time. Furthermore, the effect of

catechol on GFAP expression in astrocyte-enriched cultures obtained after a late removal of microglia was similar to changes observed in the morphology of these cells in mixed primary cultures exposed to 1 μM mercuric chloride (Cookson and Pentreath 1994). Astrocytes show highly plastic phenotypes *in vivo* (Koistinaho et al. 2004), and its activation is characterized by an increased expression of GFAP and cytoplasmic projections (Teismann and Schulz 2004). Additionally, reactive astrogliosis has become a pathological hallmark of CNS structural lesions (Sofroniew and Vinters 2010). Neuroinflammation involves the release of factors by astrocytes and microglia that act on and produce responses analogous to those of activated immune cells in the periphery (Rosales-Corral et al. 2010). However, whereas astrocytes handle an acute stress, limiting tissue damage, and restoring homeostasis, it may also inhibit adaptive neural plasticity mechanisms underlying recovery of function (Pekny and Pekna 2014). In addition, in inflammation induced by LPS, there is a dysfunctional astrocyte network, in which the actin cytoskeleton is reorganized from the normally occurring F-actin stress fibers into the more diffuse, disorganized, ring-form globular G-actin (Hansson 2015). Although reactive astrogliosis contributes to both inflammation and its resolution (Guttenplan and Liddelow 2019), astrocytes are affected in neurodegenerative diseases, such as PD, as well as neurons (Cabezas et al. 2019). This is important because neuron functions are affected by the loss of astrocytes (Baez-Jurado et al. 2019). Dopamine metabolites and reactive oxidation products may be involved in this pathological process. In this work, catechol induced more reactivity in astrocytes obtained after a late removal of microglia than in those in which these cells were removed early.

In the CNS, the expression of COMT mainly in microglia, and in a lesser extent in astrocytes (Meiser et al. 2013), constitutes a metabolic defense against catechols, but in our experiments, microglia were absent. Catechins belong to the class of flavan-3-ols that despite of their low bioavailability modulate kinase-signaling pathways in glial cells, which regulates the expression of TNF- α (Vidak et al. 2015). A catechol molecule in the class of *N*-(methyl pyridyl)thiazol-2-amines showed the more potent anti-prion activity than other tested analogs that do not bear the catechol group (Blázquez-Sánchez et al. 2017). Some fruits contain a flavonoid that carries the catechol group in its molecular structure (Figueira et al. 2017; Kujawska and Jodynys-Liebert 2018). This compound attenuated amyloid- β (A β) (1–42)-induced cytotoxicity, lipid peroxidation, and protein oxidation as well as apoptosis in primary hippocampal neuron cultures (Moeini et al. 2019). Therefore, it seems that when catechols are present in polyphenols they are less toxic or even act as protective antioxidants, depending on their structures and concentrations.

GSH increased cellularity and diminished GFAP organization in fibrillary processes only in catechol-treated astrocytes that were early isolated from microglia. GSH is an endogenous antioxidant thiol; its levels are decreased in PD patients, and its depletion induces toxic effects to cultured rat mesencephalic cells (Foley et al. 2000). The GSH depletion in astrocytes induced by buthionine sulfoximine, which inhibits its synthesis, did not kill cells (Chen et al. 2001), but they were not submitted to an OS at the same time, e.g., it occurs during catechol oxidation. GSH operates in concert with antioxidant enzymes and other low-molecular-weight antioxidant compounds to maintain redox homeostasis (Schipper 2004). Since GSH prevented catechol-induced morphological changes in astrocytes that were early separated from microglia, it was probably a consequence of an OS due to its oxidation. Low levels of GSH may render neurons vulnerable to excitotoxic and free radical damages (Nagatsu and Sawada 2005). Catechol induced a GSH depletion in neuroblastoma N2a cells, and thiols, like *N*-acetyl-cysteine and L-cysteine, protected them from its cytotoxicity (Lima et al. 2008). GSH is consumed during the action of glutathione *S*-transferase (EC 2.5.1.18) that plays a role counteracting the toxic effects elicited by neurotoxins (de Oliveira 2016), such as catechols like 6OHDA. The amino acid L-theanine, found in tea, increased GSH level in both astrocytes and glial-conditioned medium *in vitro*, as well as in the striatum of mice *in vivo*, and attenuated excess dopamine-induced neurotoxicity in neuron-astrocyte co-cultures (Deb et al. 2019).

Astrogliosis is a complex component of cellular response to injury, an important orchestrator of inflammation regulation and repair, leading to functional changes and clinical outcomes. Reactive astrocytes with hypertrophied cell bodies and thickened processes are identified in the penumbra region surrounding a spinal cord injury (Levine et al. 2016). Microglia and astrocytes also secrete insulin-degrading enzymes (EC 3.4.24.56), which enhance A β clearance (Habtariam 2018). Moreover, the presence of activated microglia and astrocytes, increased production of pro-inflammatory cytokines, and decreased anti-inflammatory ones are neuroinflammation evidences found in autism spectrum disorders (Morris et al. 2018).

The increased resistance to catechol in astrocyte-enriched cultures obtained after a late removal of microglia, as well as the inhibition of its auto-oxidation, and morphological alterations induced by it suggests that these cells modulated the responses. This hypothesis was supported by an increase in resistance to catechol of astrocyte-enriched cultures obtained after an early removal of microglia in the presence of MCM. Although the conditioned media derived from primary microglia-enriched cultures can contain neurotoxic factors (Aschner et al. 1999), these cells may also provide neuroprotection by the release of GDNF (Teismann and Schulz 2004). There is a controversy about the neuroprotective or

neurodetrimental role of lipocalin-2, an acute-phase protein that may be expressed and secreted by microglia (Ferreira et al. 2015).

In the present study, catechol induced a morphological response in astrocyte-enriched cultures in which microglia were early removed in the presence of 20% MCM. Activated microglia are found in the area associated with cell loss in PD, possibly releasing pro-inflammatory prostaglandins and cytokines, which can participate in astrocyte activation (Teismann and Schulz 2004). GFAP is upregulated in activated astroglial cells such as in retinal detachment (Nakazawa et al. 2007). Reactive astrocytes, microglia, and secreted extracellular molecules form the glial scar that surrounds the center of a spinal cord injury (Renault-Mihara et al. 2008). Increased histone deacetylase activities seem to be involved in pro-inflammatory responses. Despite the fact that microglia were not activated in the present study, “resting” microglia release basal levels of IL-1 β , IL-10, and insulin-like growth factor 1 in cultures (Xing et al. 2018).

BDNF, NGF, and GDNF are among neurotrophic factors that influence the survival and function of CNS neurons (Tuszynski and Gage 1995). In the present observations, neither early or late microglial removal nor catechol interfered in the transcription of *Gdnf*. GDNF has both a neuroprotective and restorative capacity in animal models of PD (Kuan and Barker 2005), such as following a mechanical lesion of the striatum, in which it is released by reactive astrocytes and by activated microglia, supporting neurons (Przedborski 2007). GDNF is a 134-amino-acid protein that promotes the survival and morphological differentiation of midbrain dopaminergic neurons (Abdel-Salam 2008). However, a tissue transplantation of glial cells releasing GDNF into the cerebral ventricles or basal ganglia failed to show any major clinical improvement in PD (Choonara et al. 2009). The intrastriatal injection of GDNF enhances methamphetamine- or potassium-evoked dopamine release (Cui et al. 2017). This also lowered the baseline levels of 3,4-dihydroxyphenylacetic acid and homovanillic acid after 3 weeks, which suggests a decrease in dopamine metabolism (Renko et al. 2018). GDNF is a component of the medium used to differentiate a human neuronal precursor cell line in postmitotic human dopaminergic neurons (Gutbier et al. 2018).

In the present study, the early removal of microglia increased the *Ngf* transcription in astrocyte-enriched cultures, but no effect was observed for catechol treatments. Noradrenergic β -receptors were found on polygonal astrocytes in mixed primary rat cortical cultures (Stone and Ariano 1989). Therefore, it seems that the synthesis of NGF induced by catecholamines is not due to the catechol group and its oxidation, which reinforces the idea that a noradrenergic action regulates it. IL-1 and fibroblast growth factor (FGF) also increase *Ngf* mRNA in cultured astrocytes, and since astroglia synthesize FGF (Unsicker

et al. 1992), it can be hypothesized that this protein is involved in the upregulation of *Ngf* in the absence of microglia. However, it remains to be tested. The absence of microglia represents a challenge to the CNS. The upregulation of NGF in this condition may be a response to preserve the mitochondrial membrane potential in neurons, since it declined in PC12 cells deprived of this growth factor (Foley et al. 2000). The upregulation of the *Ngf*-induced gene by twofold in the ipsilateral dorsal root ganglion in animals submitted to spinal nerve ligation (Wang et al. 2002) was lesser than the almost fivefold observed in astrocytes after an early removal of microglia in our work. NGF is decreased in nigrostriatal regions and ventricular and lumbar CSF in postmortem samples of patients with PD (Nagatsu and Sawada 2005). Therefore, it seems that the upregulation of *Ngf* in astrocytes that were early separated from microglia may represent an attempt to ask for help. NGF binds specifically to the membrane receptor TrkA, and like all neurotrophins it binds to the receptor p75 (Lykissas et al. 2007). Some authors have considered NGF as a proapoptotic protein that may represent a potential route by which reactive astrocytes may potentiate neurodegeneration via p75 receptor activation (Calkins et al. 2009). Astrocytes, together with microglia, release NGF, promoting neuroplasticity and rebuilding of the nervous system after injury (Ricci et al. 2009). Furthermore, NGF induced neurite outgrowth during PC12 cell differentiation (Rosales-Corral et al. 2010). Vectors encoding NGF have been used in a phase I clinical trial in patients with AD (Biffi et al. 2011). The regulatory elements of the amyloid precursor protein gene respond to the stimulation of NGF (Cai et al. 2011). Another possible interpretation for the upregulation of *Ngf* in astrocytes due to the early removal of microglia is the fact that this growth factor induces microglial proliferation (Gao et al. 2012). Aminochrome, which is a compound that results from dopamine oxidation, seems to downregulate *Ngf* mRNA expression in organotypic midbrain slice cultures (de Araujo et al. 2018). NGF has been used in various models of neuroprotection including cell lines, in vivo experiments, and clinical trials (Cabezas et al. 2019).

Catechol decreased *Bdnf* mRNA in astrocyte-enriched cultures in which microglia were late removed. Although BDNF is also released by activated microglia and supports the survival and process outgrowth of dopaminergic structures in the striatum (Teismann and Schulz 2004), these cells were not present at a significant amount in astrocyte-enriched cultures. There are evidences showing that other catechols also interfere in the BDNF synthesis. BDNF levels are decreased in the nigrostriatal region of postmortem brains and/or in the ventricular or lumbar CSF from patients with sporadic PD, as well as in animal models, such as 6OHDA-induced PD (Nagatsu and Sawada 2005). BDNF promotes the survival of

dopaminergic neurons in vivo (Przedborski 2007). The neuroprotective-neurorescue activity of rasagiline with application in PD is due in part to its ability to increase BDNF (Youdim et al. 2007). Astrocytes synthesize and release BDNF when activated (Rajkowska and Miguel-Hidalgo 2007). Intra-striatal delivery of the *Bdnf* gene by encoding viral vectors protected nigrostriatal dopaminergic neurons against 6OHDA (Abdel-Salam 2008). However, the immune activation of glial cells seems to downregulate BDNF, which may contribute to neurotoxicity (Choonara et al. 2009). Elevated ROS decrease BDNF-mediated synaptic plasticity (Adibhatla and Hatcher 2010). *Bdnf* is activated by Nrf2 at least in primary neuronal cultures (Tufekci et al. 2011). Indeed, BDNF has been used in various models of neuroprotection including cell lines, in vivo experiments, and clinical trials (Cabezas et al. 2019). BDNF plays a neuroprotective role under conditions of OS induced by oxygen and glucose deprivation in an ex vivo brain slice model (Gonzalez-Rodriguez et al. 2019). The protection exerted by BDNF is mediated in part by the activation of serine/threonine-specific protein kinases (EC 2.7.1.37) (Baez-Jurado et al. 2019). However, the reason why catechol decreased *Bdnf* transcription only in astrocyte-enriched cultures in which microglia were late removed is not clear and deserves more investigation.

Apparently, *Il1beta* expression was higher in astrocyte-enriched cultures in which microglia were early removed than in those obtained after a late removal. IL-1 increases both the amount of NGF present in astroglial cells and its secretion into the culture medium (Unsicker et al. 1992). Therefore, IL-1 β may be at least partially responsible for the upregulation of *Ngf* observed in astrocyte-enriched cultures in which microglia were early removed. IL-1 is present in the CSF, *Il1* mRNA is detected in normal brain, and IL-1 β -like immunoreactivity in both hypothalamic and extra-hypothalamic sites in human brain has been identified (Marchetti et al. 1995). However, it seems that the catechol group present in catecholamines and their metabolites are not responsible for this upregulation, since catechol decreased *Il1beta* expression in astrocyte-enriched cultures. IL-1 β can apparently be produced by both reactive astrocytes and activated microglia (Przedborski 2007). Catechol killed neuroblastoma N2a cells mainly by apoptosis (Lima et al. 2008). Apoptosis results from the activation of caspases. In familial amyotrophic lateral sclerosis, superoxide dismutase-1 (EC 1.15.1.1) mutations may activate caspase-1 (EC 3.4.22.36), which leads to IL-1 production that can induce a local microglial inflammatory response and affect neurons (Choonara et al. 2009). IL-1 β is important for microglial activation because it induces proliferation and immunophenotypical/functional changes in these cells (Ricci et al. 2009). Probably, *Il1beta* expression was increased in astrocyte-enriched cultures in which microglia were early removed as an attempt to recruit them.

The increase of IL-1 in PD is associated with an increase in iron levels, which increases the severity of neurological changes (Adibhatla and Hatcher 2010). Neurons also produce IL-1 (Rosales-Corral et al. 2010). Brain pericytes also produce IL-1 β (Sá-Pereira et al. 2012). Since IL-1 β can be produced by several cells of the CNS especially in neuroinflammatory conditions, it is important to know that catechol downregulates it. The biosynthesis of IL-1 β is complex, and it is regulated in multiple levels (Hansson 2015). Furthermore, in the AD brain there is production of ROS and elaboration of IL-1 β (Schipper and Song 2015). Human spinal cord astrocytes treated with IL-1 β became reactive and acquired more extensive processes formed by GFAP (Teh et al. 2017), similar with changes induced by catechol in astrocyte-enriched cultures in which microglia were late removed. The expression of IL-1 β is one functional characteristic of M1 microglia that attracts new cells of the immune system (Hornedo-Ortega et al. 2018). However, it can be neurotoxic affecting mitochondrial energetic processes in dopaminergic neurons and activation of apoptotic pathways (Cabezas et al. 2019).

Il10 transcription was higher in astrocyte-enriched cultures obtained after a late microglial removal than in those obtained after an early removal. IL-10 inhibits the expression of nitrogen oxide synthase II gene (Faraci and Heistad 1998). Both microglia and astrocytes produce IL-10 (Nagatsu and Sawada 2005). Astrocytes produce IL-10 especially during inflammation, participating in the immune response (Ricci et al. 2009). The present data suggest that astrocyte-microglial interactions are involved in the IL-10 production by astrocytes. IL-10 released by astrocytes modulates microglial activity (Rosales-Corral et al. 2010). During the inflammatory processes, secretion of IL-10 leads to neutralization of activated macrophages (Calabrese et al. 2010). Probably the transcription of *Il10* in astrocyte-enriched cultures obtained after a late microglial removal is a way for signaling to microglia “You are welcome, stay in peace.” This signaling changes during inflammatory conditions. The transcription of *Il10* increased in LPS-treated purified microglia, but not in astrocyte monocultures (Kim et al. 2011). In AD, there is usually an IL-10 decrease (Cai et al. 2011). Catechol decreased the *Il10* expression in astrocyte-enriched cultures obtained after a late removal of microglia. The orthoquinone tanshinone I administered to male C57BL/6 mice also decreased IL-10 in MPTP-challenged animals (Kujawska and Jodynis-Liebert 2018). IL-10 is an immunosuppressive molecule that contributes to control inflammation and is essential for wound healing (Baez-Jurado et al. 2019).

Astrocytes that remained in contact with microglial cells for 7 to 10 days before their isolation were more resistant to catechol-induced cytotoxicity than those that were separated from microglia 48 h after the plating of primary mixed

cultures. The resistance was also observed for astrocytes obtained after an early removal of microglia when these cells were incubated in the presence of MCM. MCM not only protected astrocytes; it also inhibited catechol oxidation. Astrocytes isolated after a late removal of microglia presented changes in their morphology when exposed to catechol similar to those observed for astrocytes obtained after an early removal of microglia, but that were incubated with MCM. Therefore, these data confirm the hypothesis that astrocytes early separated from microglia in cultures present different responses in injury caused by catechol in comparison to those that stayed with microglia for a longer time. Furthermore, astrocytes that were isolated after an early removal of microglia expressed more *Il1beta* and *Ngf*, probably as an attempt to recruit cells from the immune system. On the contrary, astrocytes that were isolated after a late removal of microglia expressed more *Il10* as if they were signaling to them “You are welcome, stay in peace!” Catechol decreased *Bdnf* and *Il10* in astrocyte cultures in which microglia were late removed, and it decreased the expression of *Il1beta* in both conditions. These data are important because it increases knowledge about the cytotoxicity of catechol molecules and their effects on glial cells. Probably, interactions between astrocytes and microglia contribute to protect the CNS against the toxic effects of endogenous and exogenous catechol molecules. This is also an alert for studies carried out in in vitro testing the effect of drugs in primary cultures of cells isolated from the CNS. These studies must take care of limitations of these models, since interactions among different cells that occurs in vivo may modify responses.

Acknowledgements The authors thank The Brazilian National Council of Scientific and Technological Development (CNPq) for the doctorate scholarship to J.M.P.B., and for productivity fellowships to S.L.C., M.F.D.C., and R.S.E. The authors wish to thank the Program for Technological Development in Tools for Health-PDTIS-FIOCRUZ for the use of Confocal Microscopy Service IPqGM facilities.

Author Contribution Conceptualization, R.S.E.; methodology, J.M.P.B., V.D.A.S., S.L.C., M.F.D.C., and R.S.E.; investigation, J.M.P.B., L.B.J., C.S.S., and R.S.E.; formal analysis, J.M.P.B., L.B.J., R.S.E.; resources, V.D.A.S., S.L.C., M.F.D.C., and R.S.E.; writing — original draft, J.M.P.B. and R.S.E.; writing — review and editing, J.M.P.B., C.S.S., V.D.A.S., S.L.C., M.F.D.C., and R.S.E.; visualization, J.M.P.B., C.S.S.; supervision, R.S.E.; project administration, R.S.E.; funding acquisition, R.S.E.

Funding This research was supported by the Brazilian National Council of Scientific and Technological Development (CNPq), project grant Universal 447806/2014–9 to Ramon dos Santos El-Bachá. The funding source had no role in the study design; in the collection, analysis, and interpretation of data; in the writing of the report; and in the decision to submit the article for publication.

Data Availability The data that support the findings of this study are archived in Gin and will be open available upon acceptance of this research manuscript.

Declarations

Conflict of Interest The authors declare no competing interests.

References

- Abdel-Salam OME (2008) Drugs used to treat Parkinson's disease, present status and future directions. *CNS & Neurological Disorders - Drug Targets- CNS & Neurological Disorders* 7(4):321–342
- Adibhatla RM, Hatcher JF (2010) Lipid oxidation and peroxidation in CNS health and disease: from molecular mechanisms to therapeutic opportunities. *Antioxid Redox Signal* 12:125+
- Almeida WLC, Vitor DN, Pereira MRG, De Sa DS, Alvarez LDG, Pinheiro AM, El-Bacha RS (2007) Redox properties of ruthenium complex with catechol are involved in toxicity to glial cells. *J Chil Chem Soc* 52(3):1240–1243
- Amtul Z, Hepburn JD (2014) Protein markers of cerebrovascular disruption of neurovascular unit: immunohistochemical and imaging approaches. In *Reviews in the Neurosciences* 25:481
- Arai K, Lee SR, Lo EH (2003) Essential role for ERK mitogen-activated protein kinase in matrix metalloproteinase-9 regulation in rat cortical astrocytes. *Glia* 43(3):254–264. <https://doi.org/10.1002/glia.10255>
- Aschner M, Allen JW, Kimelberg HK, LoPachin RM, Streit WJ (1999) Glial cells in neurotoxicity development. *Annu Rev Pharmacol Toxicol* 39(1):151
- Baez-Jurado E, Hidalgo-Lanussa O, Barrera-Bailón B, Sahebkar A, Ashraf GM, Echeverria V, Barreto GE (2019) Secretome of mesenchymal stem cells and its potential protective effects on brain pathologies. *Mol Neurobiol* 56(10):6902–6927. <https://doi.org/10.1007/s12035-019-1570-x>
- Ballabh P, Braun A, Nedergaard M (2004) The blood-brain barrier: an overview: structure, regulation, and clinical implications. *Neurobiol Dis* 16(1):1–13. <https://doi.org/10.1016/j.nbd.2003.12.016>
- Barreto GES, dos Santos GS, Egito EST, El-Bachá RS (2005) Catechol inhibits FADH₂-linked respiration in rat liver mitochondrial fraction. *Acta Cirúrgica Brasileira* 20(Supl 1):40–45
- Barreto GES, Oliveira ESd, Villar FAGAd, Santos GSd, Lima RMF, Costa SL, El-Bachá RS (2007) Investigation of toxic factors affecting cells of rat brains exposed to 3-methylcatechol. *Braz Arch Biol Technol* 50:839–849
- Belous AR, Hachey DL, Dawling S, Roodi N, Parl FF (2007) Cytochrome P450 1B1-mediated estrogen metabolism results in estrogen-deoxyribonucleoside adduct formation. *Cancer Res* 67(2):812–817. <https://doi.org/10.1158/0008-5472.can-06-2133>
- Biffi A, Aubourg P, Cartier N (2011) Gene therapy for leukodystrophies. *Hum Mol Genet* 20(R1):R42–R53
- Blázquez-Sánchez MT, De Matos AM, Rauter AP (2017) Exploring anti-prion glyco-based and aromatic scaffolds: a chemical strategy for the quality of life. *Molecules* 22(6):864
- Bohlen CJ, Bennett FC, Tucker AF, Collins HY, Mulinyawe SB, Barres BA (2017) Diverse requirements for microglial survival, specification, and function revealed by defined-medium cultures. *Neuron* 94(4):759–773.e758. <https://doi.org/10.1016/j.neuron.2017.04.043>
- Cabezas R, Baez-Jurado E, Hidalgo-Lanussa O, Echeverria V, Ashraf GM, Sahebkar A, Barreto GE (2019) Growth factors and neuroglobin in astrocyte protection against neurodegeneration and oxidative stress. *Mol Neurobiol* 56(4):2339–2351. <https://doi.org/10.1007/s12035-018-1203-9>
- Cai Z, Zhao B, Ratka A (2011) Oxidative stress and β -amyloid protein in Alzheimer's disease. *NeuroMol Med* 13(4):223–250. <https://doi.org/10.1007/s12017-011-8155-9>








- Caito S, Yu Y, Aschner M (2013) Differential response to acrylonitrile toxicity in rat primary astrocytes and microglia. *Neurotoxicology* 37:93–99. <https://doi.org/10.1016/j.neuro.2013.04.007>
- Calabrese V, Cornelius C, Dinkova-Kostova AT, Calabrese EJ, Mattson MP (2010) Cellular stress responses, the hormesis paradigm, and vitagenes: novel targets for therapeutic intervention in neurodegenerative disorders. *Antioxid Redox Signal* 13:1763+
- Calkins MJ, Johnson DA, Townsend JA, Vargas MR, Dowell JA, Williamson TP, Johnson JA (2009) The Nrf2/ARE pathway as a potential therapeutic target in neurodegenerative disease. *Antioxid Redox Signal* 11:497+
- Chen C, Kong X, Lee I-S (2015) Modification of surface/neuron interfaces for neural cell-type specific responses: a review. *Biomed Mater* 11(1):014108. <https://doi.org/10.1088/1748-6041/11/1/014108>
- Chen Y, Vartiainen NE, Ying W, Chan PH, Koistinaho J, Swanson RA (2001) Astrocytes protect neurons from nitric oxide toxicity by a glutathione-dependent mechanism. *J Neurochem* 77(6):1601–1610. <https://doi.org/10.1046/j.1471-4159.2001.00374.x>
- Choonara YE, Pillay V, Du Toit LC, Modi G, Naidoo D, Ndesendo VMK, Sibambo SR (2009) Trends in the molecular pathogenesis and clinical therapeutics of common neurodegenerative disorders. *Int J Mol Sci* 10(6):2510–2557
- Cookson MR, Pentreath VW (1994) Alterations in the glial fibrillary acidic protein content of primary astrocyte cultures for evaluation of glial cell toxicity. *Toxicol in Vitro* 8(3):351–359
- Cui X, Gooch H, Petty A, McGrath JJ, Eyles D (2017) Vitamin D and the brain: genomic and non-genomic actions. *Mol Cell Endocrinol* 453:131–143. <https://doi.org/10.1016/j.mce.2017.05.035>
- de Araujo FM, Ferreira RS, Souza CS, Dos Santos CC, Rodrigues TLRS, Silva JHC, Silva VDA (2018) Aminochrome decreases NGF, GDNF and induces neuroinflammation in organotypic mid-brain slice cultures. *Neurotoxicology* 66:98–106. <https://doi.org/10.1016/j.neuro.2018.03.009>
- de Oliveira DM, Pitanga BPS, Grangeiro MS, Lima RMF, Costa MFD, Costa SL, El-Bacha RS (2010) Catechol cytotoxicity in vitro: induction of glioblastoma cell death by apoptosis. *Hum Exp Toxicol* 29(3):199–212. <https://doi.org/10.1177/0960327109360364>
- de Oliveira MR (2016) The dietary components carnosic acid and carnosol as neuroprotective agents: a mechanistic view. *Mol Neurobiol* 53(9):6155–6168. <https://doi.org/10.1007/s12035-015-9519-1>
- Deb S, Dutta A, Phukan BC, Manivasagam T, Justin Thenmozhi A, Bhattacharya P, Borah A (2019) Neuroprotective attributes of L-theanine, a bioactive amino acid of tea, and its potential role in Parkinson's disease therapeutics. *Neurochem Int* 129:104478. <https://doi.org/10.1016/j.neuint.2019.104478>
- El-Bachá RS, Daval JL, Koziel V, Netter P, Minn A (2001) Toxic effects of apomorphine on rat cultured neurons and glial C6 cells, and protection with antioxidants. *Biochem Pharmacol* 61(1):73–85
- El-Bachá RS, Netter P, Minn A (1999) Mechanisms of apomorphine cytotoxicity towards rat glioma C6 cells: protection by bovine serum albumin and formation of apomorphine-protein conjugates. *Neurosci Lett* 263(1):25–28. [https://doi.org/10.1016/s0304-3940\(99\)00088-9](https://doi.org/10.1016/s0304-3940(99)00088-9)
- Eldahshan W, Fagan SC, Ergul A (2019) Inflammation within the neurovascular unit: focus on microglia for stroke injury and recovery. *Pharmacol Res* 147:104349. <https://doi.org/10.1016/j.phrs.2019.104349>
- Faraci FM, Heistad DD (1998) Regulation of the cerebral circulation: role of endothelium and potassium channels. *Physiol Rev* 78(1):53–97. <https://doi.org/10.1152/physrev.1998.78.1.53>
- Ferreira AC, Dá Mesquita S, Sousa JC, Correia-Neves M, Sousa N, Palha JA, Marques F (2015) From the periphery to the brain: Lipocalin-2, a friend or foe? *Prog Neurobiol* 131:120–136. <https://doi.org/10.1016/j.pneurobio.2015.06.005>
- Figueira I, Garcia G, Pimpão RC, Terrasso AP, Costa I, Almeida AF, Santos CN (2017) Polyphenols journey through blood-brain barrier towards neuronal protection. *Sci Rep* 7(1):11456. <https://doi.org/10.1038/s41598-017-11512-6>
- Floden AM, Combs CK (2007) Microglia repetitively isolated from in vitro mixed glial cultures retain their initial phenotype. *J Neurosci Methods* 164(2):218–224. <https://doi.org/10.1016/j.jneumeth.2007.04.018>
- Foley P, Gerlach M, Youdim MBH, Riederer P (2000) MAO-B inhibitors: multiple roles in the therapy of neurodegenerative disorders? *Parkinsonism Relat Disord* 6(1):25–47. [https://doi.org/10.1016/S1353-8020\(99\)00043-7](https://doi.org/10.1016/S1353-8020(99)00043-7)
- Gao H-M, Zhou H, Hong J-S (2012) NADPH oxidases: novel therapeutic targets for neurodegenerative diseases. *Trends Pharmacol Sci* 33(6):295–303. <https://doi.org/10.1016/j.tips.2012.03.008>
- Ghatak S, Trudler D, Dolatabadi N, Ambasadhan R (2018) Parkinson's disease: what the model systems have taught us so far. *J Genet* 97(3):729–751
- Gonzalez-Rodriguez P, Ugidos IF, Perez-Rodriguez D, Anuncibay-Soto B, Santos-Galdiano M, Font-Belmonte E, Fernandez-Lopez A (2019) Brain-derived neurotrophic factor alleviates the oxidative stress induced by oxygen and glucose deprivation in an ex vivo brain slice model. *J Cell Physiol* 234(6):9592–9604. <https://doi.org/10.1002/jcp.27646>
- Gutierrez S, Spreng A-S, Delp J, Schildknecht S, Karreman C, Suci I, Leist M (2018) Prevention of neuronal apoptosis by astrocytes through thiol-mediated stress response modulation and accelerated recovery from proteotoxic stress. *Cell Death Differ* 25(12):2101–2117. <https://doi.org/10.1038/s41418-018-0229-x>
- Guttenplan KA, Liddel SA (2019) Astrocytes and microglia: models and tools. *J Exp Med* 216(1):71–83. <https://doi.org/10.1084/jem.20180200>
- Habtemariam S (2018) Iridoids and other monoterpenes in the Alzheimer's brain: recent development and future prospects. *Molecules* 23(1):117
- Hansson E (1984) Cellular composition of a cerebral hemisphere primary culture. *Neurochem Res* 9(2):153–172. <https://doi.org/10.1007/bf00964164>
- Hansson E (2015) Actin filament reorganization in astrocyte networks is a key functional step in neuroinflammation resulting in persistent pain: novel findings on network restoration. *Neurochem Res* 40(2):372–379. <https://doi.org/10.1007/s11064-014-1363-6>
- Hornedo-Ortega R, Cerezo AB, de Pablos RM, Krisa S, Richard T, García-Parrilla MC, Troncoso AM (2018) Phenolic compounds characteristic of the Mediterranean diet in mitigating microglia-mediated neuroinflammation. *Front Cell Neurosci* 12(373). <https://doi.org/10.3389/fncel.2018.00373>
- Hughes JB, Sousa JS, Barreto RA, Silva AR, Souza CS, Silva VDA, Costa SL (2005) Cytotoxic effects of an extract containing alkaloids obtained from *Prosopis juliflora* Sw. D.C. (Algaroba) pods on glioblastoma cells. *Revista Brasileira de Saúde e Produção Animal* 6(1):31–41
- Ito S, Yamanaka Y, Ojika M, Wakamatsu K (2016) The metabolic fate of ortho-quinones derived from catecholamine metabolites. *Int J Mol Sci* 17(2). <https://doi.org/10.3390/ijms17020164>
- Janda E, Isidoro C, Carresi C, Mollace V (2012) Defective autophagy in Parkinson's disease: role of oxidative stress. *Mol Neurobiol* 46(3):639–661. <https://doi.org/10.1007/s12035-012-8318-1>
- Jiang L, Chen SH, Chu CH, Wang SJ, Oyarzabal E, Wilson B, Hong JS (2015) A novel role of microglial NADPH oxidase in mediating extra-synaptic function of norepinephrine in regulating brain immune homeostasis. *Glia* 63(6):1057–1072. <https://doi.org/10.1002/glia.22801>
- Juricek L, Coumoul X (2018) The aryl hydrocarbon receptor and the nervous system. *Int J Mol Sci* 19(9):2504
- Kim S, Kim YE, Hong S, Kim KT, Sung DK, Lee Y, Song MR (2019) Reactive microglia and astrocytes in neonatal intraventricular

- hemorrhage model are blocked by mesenchymal stem cells. *Glia*. <https://doi.org/10.1002/glia.23712>
- Kim S, Steelman AJ, Koito H, Li J (2011) Astrocytes promote TNF-mediated toxicity to oligodendrocyte precursors. *J Neurochem* 116(1):53–66. <https://doi.org/10.1111/j.1471-4159.2010.07084.x>
- Koistinaho M, Lin S, Wu X, Esterman M, Koger D, Hanson J, Paul SM (2004) Apolipoprotein E promotes astrocyte colocalization and degradation of deposited amyloid- β peptides. *Nat Med* 10(7):719–726. <https://doi.org/10.1038/mm1058>
- Kuan WL, Barker RA (2005) New therapeutic approaches to Parkinson's disease including neural transplants. *Neurorehabil Neural Repair* 19:155
- Kujawska M, Jodynis-Liebert J (2018) Polyphenols in Parkinson's disease: a systematic review of in vivo studies. *Nutrients* 10(5):642
- Lai C-T, Yu PH (1997) Dopamine- and 1- β -3,4-dihydroxyphenylalanine hydrochloride (L-Dopa)-induced cytotoxicity towards catecholaminergic neuroblastoma SH-SY5Y cells: effects of oxidative stress and antioxidative factors. *Biochem Pharmacol* 53(3):363–372. [https://doi.org/10.1016/S0006-2952\(96\)00731-9](https://doi.org/10.1016/S0006-2952(96)00731-9)
- Lange SC, Bak LK, Waagepetersen HS, Schousboe A, Norenberg MD (2012) Primary cultures of astrocytes: their value in understanding astrocytes in health and disease. *Neurochem Res* 37(11):2569–2588. <https://doi.org/10.1007/s11064-012-0868-0>
- Levine J, Kwon E, Paez P, Yan W, Czerwiec G, Loo JA, Wanner IB (2016) Traumatically injured astrocytes release a proteomic signature modulated by STAT3-dependent cell survival. *Glia* 64(5):668–694. <https://doi.org/10.1002/glia.22953>
- Lima RMF, Alvarez LDG, Costa MFD, Costa SL, Clarencio J, El-Bacha RS (2008) Cytotoxic effects of catechol to neuroblastoma N2a cells. *Gen Physiol Biophys* 27(4):306–314
- Losciuto S, Dorban G, Gabel S, Gustin A, Hoenen C, Grandbarbe L, Heurtaux T (2012) An efficient method to limit microglia-dependent effects in astroglial cultures. *J Neurosci Methods* 207(1):59–71. <https://doi.org/10.1016/j.jneumeth.2012.03.010>
- Lykissas MG, Batistatou AK, Charalabopoulos KA, Beris AE (2007) The role of neurotrophins in axonal growth, guidance, and regeneration. *Curr Neurovasc Res* 4(2):143–151
- Marchetti B, Morale MC, Gallo F, Batticane N, Farinella Z, Cioni M (1995) Neuroendocrineimmunology (NEI) at the turn of the century: towards a molecular understanding of basic mechanisms and implications for reproductive physiopathology. *Endocrine* 3(12):845–861. <https://doi.org/10.1007/bf02738890>
- Mecha M, Iñigo PM, Mestre L, Hernangómez M, Borrell J, Guaza C (2011) An easy and fast way to obtain a high number of glial cells from rat cerebral tissue: a beginners approach
- Meiser J, Weindl D, Hiller K (2013) Complexity of dopamine metabolism. *Cell Communication and Signaling* 11
- Mesquita SD, Ferreira AC, Falcao AM, Sousa JC, Oliveira TG, Correia-Neves M, Palha JA (2014) Lipocalin 2 modulates the cellular response to amyloid beta. *Cell Death Differ* 21(10):1588–1599. <https://doi.org/10.1038/cdd.2014.68>
- Moeini R, Memariani Z, Asadi F, Bozorgi M, Gorji N (2019) Pistacia genus as a potential source of neuroprotective natural products. *Planta Med* 85(17):1326–1350. <https://doi.org/10.1055/a-1014-1075>
- Morris G, Puri BK, Frye RE, Maes M (2018) The putative role of environmental mercury in the pathogenesis and pathophysiology of autism spectrum disorders and subtypes. *Mol Neurobiol* 55(6):4834–4856. <https://doi.org/10.1007/s12035-017-0692-2>
- Mosmann T (1983) Rapid colorimetric assay for cellular growth and survival: application to proliferation and cytotoxicity assays. *J Immunol Methods* 65(1–2):55–63
- Nagatsu T, Sawada M (2005) Inflammatory process in Parkinsons disease: role for cytokines. *Curr Pharm Des* 11(8):999–1016. <https://doi.org/10.2174/1381612053381620>
- Nakazawa T, Takeda M, Lewis GP, Cho KS, Jiao J, Wilhelmsson U, Miller JW (2007) Attenuated glial reactions and photoreceptor degeneration after retinal detachment in mice deficient in glial fibrillary acidic protein and vimentin. *Invest Ophthalmol vis Sci* 48(6):2760–2768. <https://doi.org/10.1167/iovs.06-1398>
- Noble PG, Antel JP, Yong VW (1994) Astrocytes and catalase prevent the toxicity of catecholamines to oligodendrocytes. *Brain Res* 633(1):83–90. [https://doi.org/10.1016/0006-8993\(94\)91525-3](https://doi.org/10.1016/0006-8993(94)91525-3)
- Norden DM, Trojanowski PJ, Walker FR, Godbout JP (2016) Insensitivity of astrocytes to interleukin 10 signaling following peripheral immune challenge results in prolonged microglial activation in the aged brain. *Neurobiol Aging* 44:22–41. <https://doi.org/10.1016/j.neurobiolaging.2016.04.014>
- Pekny M, Pekna M (2014) Astrocyte reactivity and reactive astrogliosis: costs and benefits. *Physiol Rev* 94(4):1077–1098. <https://doi.org/10.1152/physrev.00041.2013>
- Pereira MRG, de Oliveira ES, de Villar FAGA, Grangeiro MS, Fonseca J, Silva AR, El-Bachá RS (2004) Cytotoxicity of catechol towards human glioblastoma cells via superoxide and reactive quinones generation. *J Bras Patol Med Lab* 40(4):280–285
- Potjewyd G, Moxon S, Wang T, Domingos M, Hooper NM (2018) Tissue engineering 3D neurovascular units: a biomaterials and bioprinting perspective. *Trends Biotechnol* 36(4):457–472. <https://doi.org/10.1016/j.tibtech.2018.01.003>
- Przedborski S (2007) Neuroinflammation and Parkinson's disease. *Handb Clin Neurol* 83:535–551. Elsevier
- Rae CD (2014) A guide to the metabolic pathways and function of metabolites observed in human brain 1H magnetic resonance spectra. *Neurochem Res* 39(1):1–36. <https://doi.org/10.1007/s11064-013-1199-5>
- Rajkowska G, Miguel-Hidalgo JJ (2007) Gliogenesis and glial pathology in depression. *CNS & Neurological Disorders - Drug Targets - CNS & Neurological Disorders* 6(3):219–233
- Renault-Mihara F, Okada S, Shibata S, Nakamura M, Toyama Y, Okano H (2008) Spinal cord injury: emerging beneficial role of reactive astrocytes' migration. *Int J Biochem Cell Biol* 40(9):1649–1653. <https://doi.org/10.1016/j.biocel.2008.03.009>
- Renko J-M, Bäck S, Voutilainen MH, Piepponen TP, Reenilä I, Saarma M, Tuominen RK (2018) Mesencephalic astrocyte-derived neurotrophic factor (MANF) elevates stimulus-evoked release of dopamine in freely-moving rats. *Mol Neurobiol* 55(8):6755–6768. <https://doi.org/10.1007/s12035-018-0872-8>
- Ricci G, Volpi L, Pasquali L, Petrozzi L, Siciliano G (2009) Astrocyte–neuron interactions in neurological disorders. *J Biol Phys* 35(4):317–336. <https://doi.org/10.1007/s10867-009-9157-9>
- Rosales-Corral S, Reiter RJ, Tan D-X, Ortiz GG, Lopez-Armas G (2010) Functional aspects of redox control during neuroinflammation. *Antioxid Redox Signal* 13:193+
- Santos CC, Araujo FM, Ferreira RS, Silva VB, Silva JHC, Grangeiro MS, Silva VDA (2017) Aminochrome induces microglia and astrocyte activation. *Toxicol in Vitro* 42:54–60. <https://doi.org/10.1016/j.tiv.2017.04.004>
- Sarrazy V, Vedrenne N, Bordeau N, Billet F, Cardot P, Desmouliere A, Battu S (2013) Fast astrocyte isolation by sedimentation field flow fractionation. *J Chromatogr A* 1289:88–93. <https://doi.org/10.1016/j.chroma.2013.03.029>
- Saura J (2007) Microglial cells in astroglial cultures: a cautionary note. *J Neuroinflammation* 4:26. <https://doi.org/10.1186/1742-2094-4-26>
- Schildge S, Bohrer C, Beck K, Schachtrup C (2013) Isolation and culture of mouse cortical astrocytes. *J Vis Exp* (71). <https://doi.org/10.3791/50079>
- Schipper HM (2004) Brain iron deposition and the free radical-mitochondrial theory of ageing. *Ageing Res Rev* 3(3):265–301. <https://doi.org/10.1016/j.arr.2004.02.001>
- Schipper HM, Song W (2015) A heme oxygenase-1 transducer model of degenerative and developmental brain disorders. *Int J Mol Sci* 16(3):5400–5419

- Schipper HM, Wang E, Snyder DS (1998) 16 - astrocyte senescence and the pathogenesis of Parkinson's disease. Handbook of the Aging Brain. Academic Press, San Diego, pp 243–257
- Schmittgen TD, Livak KJ (2008) Analyzing real-time PCR data by the comparative C(T) method. *Nat Protoc* 3(6):1101–1108
- Seki M, Tanaka T, Sakai Y, Fukuchi T, Abe H, Nawa H, Takei N (2005) Müller cells as a source of brain-derived neurotrophic factor in the retina: noradrenaline upregulates brain-derived neurotrophic factor levels in cultured rat Müller cells. *Neurochem Res* 30:1163. <https://doi.org/10.1007/s11064-005-7936-7>
- Shin JY, Ahn Y-H, Paik M-J, Park HJ, Sohn YH, Lee PH (2012) Elevated homocysteine by levodopa is detrimental to neurogenesis in Parkinsonian model. *PLoS ONE* 7(11):1–11. <https://doi.org/10.1371/journal.pone.0050496>
- Sidoryk-Wegrzynowicz M, Lee E, Mingwei N, Aschner M (2011) Disruption of astrocytic glutamine turnover by manganese is mediated by the protein kinase C pathway. *Glia* 59(11):1732–1743. <https://doi.org/10.1002/glia.21219>
- Silva VDA, Pitanga BPS, Nascimento RP, Souza CS, Coelho PLC, Menezes N, Costa SL (2013) Juliprosopine and juliprosine from *Prosopis juliflora* leaves induce mitochondrial damage and cytoplasmic vacuolation on cocultured glial cells and neurons. *Chem Res Toxicol* 26(12):1810–1820. <https://doi.org/10.1021/tx4001573>
- Sofroniew MV, Vinters HV (2010) Astrocytes: biology and pathology. *Acta Neuropathol* 119(1):7–35. <https://doi.org/10.1007/s00401-009-0619-8>
- Steelman AJ, Smith R 3rd, Welsh CJ, Li J (2013) Galectin-9 protein is up-regulated in astrocytes by tumor necrosis factor and promotes encephalitogenic T-cell apoptosis. *J Biol Chem* 288(33):23776–23787. <https://doi.org/10.1074/jbc.M113.451658>
- Stone EA, Ariano MA (1989) Are glial cells targets of the central noradrenergic system? A review of the evidence. *Brain Res Rev* 14(4):297–309. [https://doi.org/10.1016/0165-0173\(89\)90015-5](https://doi.org/10.1016/0165-0173(89)90015-5)
- Sá-Pereira I, Brites D, Brito MA (2012) Neurovascular unit: a focus on pericytes. *Mol Neurobiol* 45(2):327–347. <https://doi.org/10.1007/s12035-012-8244-2>
- Teh DBL, Prasad A, Jiang W, Ariffin MZ, Khanna S, Belorkar A, All AH (2017) Transcriptome analysis reveals neuroprotective aspects of human reactive astrocytes induced by interleukin 1 β . *Sci Rep* 7(1):13988. <https://doi.org/10.1038/s41598-017-13174-w>
- Teismann P, Schulz JB (2004) Cellular pathology of Parkinson's disease: astrocytes, microglia and inflammation. *Cell Tissue Res* 318(1):149–161. <https://doi.org/10.1007/s00441-004-0944-0>
- Thurgur H, Pinteaux E (2019) Microglia in the neurovascular unit: blood–brain barrier–microglia interactions after central nervous system disorders. *Neuroscience* 405:55–67. <https://doi.org/10.1016/j.neuroscience.2018.06.046>
- Tufekci KU, Civi Bayin E, Genc S, Genc K (2011) The Nrf2/ARE pathway: a promising target to counteract mitochondrial dysfunction in Parkinson's disease. *Parkinson's Disease* 2011. <https://doi.org/10.4061/2011/314082>
- Tuszynski MH, Gage FH (1995) Maintaining the neuronal phenotype after injury in the adult CNS. Neurotrophic factors, axonal growth substrates, and gene therapy. *Mol Neurobiol* 10(2–3):151–167. <https://doi.org/10.1007/bf02740673>
- Unsicker K, Grothe C, Westermann R, Wewetzer K (1992) Cytokines in neural regeneration. *Curr Opin Neurobiol* 2(5):671–678. [https://doi.org/10.1016/0959-4388\(92\)90037-L](https://doi.org/10.1016/0959-4388(92)90037-L)
- Vidak M, Rozman D, Komel R (2015) Effects of flavonoids from food and dietary supplements on glial and glioblastoma multiforme cells. *Molecules* 20(10):19406–19432
- Wang H, Sun H, Della Penna K, Benz RJ, Xu J, Gerhold DL, Koblan KS (2002) Chronic neuropathic pain is accompanied by global changes in gene expression and shares pathobiology with neurodegenerative diseases. *Neuroscience* 114(3):529–546. [https://doi.org/10.1016/S0306-4522\(02\)00341-X](https://doi.org/10.1016/S0306-4522(02)00341-X)
- Xing C, Li W, Deng W, Ning M, Lo EH (2018) A potential gliovascular mechanism for microglial activation: differential phenotypic switching of microglia by endothelium versus astrocytes. *J Neuroinflammation* 15(1):143. <https://doi.org/10.1186/s12974-018-1189-2>
- Youdim MBH, Riederer PF, Koller WC, Melamed E (2007) Monoamine oxidase A and B inhibitors in Parkinson's disease. *Handb Clin Neurol* 84:93–120. Elsevier
- Zafar KS, Siegel D, Ross D (2006) A potential role for cyclized quinones derived from dopamine, DOPA, and 3,4-dihydroxyphenylacetic acid in proteasomal inhibition. *Mol Pharmacol* 70(3):1079–1086. <https://doi.org/10.1124/mol.106.024703>

Publisher's Note Springer Nature remains neutral with regard to jurisdictional claims in published maps and institutional affiliations.

Authors and Affiliations

Julita Maria Pereira Borges^{1,2}  · Lívia Bacelar de Jesus¹  · Cleide dos Santos Souza¹  · Victor Diogenes Amaral da Silva¹  · Silvia Lima Costa¹  · Maria de Fátima Dias Costa¹  · Ramon Santos El-Bachá¹ 

¹ Department of Biochemistry and Biophysics, Institute of Health Sciences, Federal University of Bahia (UFBA), 40.110-902, Salvador, Bahia (BA), Brazil

² Department of Science and Technology, Southwest Bahia State University (UESB), 45.208-409, Jequié, BA, Brazil